2016

Effects of the ground heat flux on snowpack ablation in a semi-arid mountain climate

Chad Mickschl

Effects of the Ground Heat Flux on Snowpack Ablation in a Semi-Arid Mountain Climate

By

Chad Mickschl

Committee
Dr. Mark Stone, Chair
Dr. Dave Gutzler
Dr. Bruce Thomson

A Professional Project Report Submitted in Partial Fulfillment
Of the Requirements for the Degree of

Master of Water Resources
Hydroscience Concentration

Water Resources Program
The University of New Mexico
Albuquerque, New Mexico
September 2016

Abstract

In anticipation of warmer temperatures, receding snowlines, and increasing water demands, it will be important for water managers to understand how changes in snowpack depth and distribution will affect available runoff. Mountain snowpacks make up the largest component of runoff in mountain regions generating water supply for a host of downstream users. As climate warming persists, mountainous areas with traditionally deeper snowpacks will shift towards a shallower, more transitional regime. Transitional lower elevation snowpacks will begin to experience an increasing number of melt-off and ripening periods throughout the course of a winter.

To better predict changes in water resources, it is necessary to gain a more detailed knowledge of the snowmelt energy balance of shallow snow as well as quantification of lower elevation snowline energy fluxes. Typically, the ground heat flux (G) is assumed to be very small compared to other energy fluxes incident the snowpack. To understand snowpack processes, this research aims to (1) assess the contribution of the ground heat flux in the Jemez Mountains compared to other mountain regions using the SNOBAL model, (2) compare calculated and modeled ground heat flux values, and (3) determine if near surface ground temperatures can be used as an indicator of snowpack ripening and presence.

To capture the energy fluxes of the snowpack, two weather stations were deployed within the Alamo Creek Watershed on a north aspect at 9800ft and a south aspect at 8600ft. To capture and quantify the energy fluxes beneath the snowpack, near surface soil temperatures were recorded for the duration of the snow-covered season with HOBO temperature sensors. The data recorded by these temperature sensors were used to calculate the ground heat flux as well as determine snowpack ripening and day of melt.

Near surface ground temperatures at 2cm were above 0℃ during the duration of the snow covered season. G fluxes increased slightly as snowpack depth increased and more significantly during snow depths less than 25cm towards the end of the snow covered season. Seasonal ground heat flux accounted for 26% of the snowpack ablation. Snowpack modeling with typically assumed 0℃ ground temperatures resulted in snowpacks that did not melt by the observed melt date indicating that the G flux is more significant in this semi-arid mountain region. Near surface soil temperatures allowed the determination of snowpack presence and disappearance, however the ripening dates were less certain.

TABLE OF CONTENTS

Acknowledgements

This research would not have been possible without help and support from various people and agencies. First, my research would not have been possible without a grant from the New Mexico Water Resources Research Institute. This grant allowed for purchasing of additional equipment needed to conduct the research I was interested in. Second, the Valles Caldera National Preserve was essential in allowing this research to occur within their jurisdiction.

The large effort that was put into this heavily based field project also would not have been possible without the help of other students. Angela Gregory (Phd. Candidate in Civil Engineering) was essential in helping setup weather stations and programming as well as helping with using the SNOBAL model. Chase Stearnes (Undergrad Civil Engineering) was essential in spending 2 days per month all winter long in the remote Jemez Mountains helping with data collection. Other people that helped collect data in the Jemez Mountains were my dad Bill Mickschl and my wife Sarah Mickschl.

Mark Stone, my committee chair was always there to help when I had questions and could always give crucial suggestions. Dave Gutzler and Bruce Thomson were two of my committee members and always provided feedback and insights on my writing and methods.

A special thanks is in order to my family. To my Dad and Cindy for providing support and a home away from home while pursuing my masters, I couldn't have done this without them. Finally, my wife Sarah and kids Cooper and Tyler, for their patience, help, and unequivocal support during this process. I could not have finished this project without the help and dedication from them.

1. INTRODUCTION

In the mountain regions of western North America snowpacks act as reservoirs of water storage for downstream users. Mountain snowpacks make up the largest component of runoff in these regions generating water supply for a host of downstream uses such as municipalities, agriculture, terrestrial and aquatic ecosystems, and recreation.

Average surface temperatures in the western US have increased over 1°C to 2°C over the last 20 years (Intergovernmental Panel on Climate Change, 2013). Temperatures in Arizona and New Mexico have been rising, particularly since the mid-1970s. Since 1976, the average annual temperature increased by 2.5°F in Arizona and 1.8°F in New Mexico (Lenart, 2008). Climate models forecast air temperatures in New Mexico to increase by 6-12°F on average (Allen *et al.*, 2005). These increases are also projected to be more pronounced in winter, and at high elevations. More episodes of extreme heat, fewer episodes of extreme cold, longer frost-free seasons, and winter precipitation falling more often as rain will all impact water availability in this region.

Climate models suggest that warming temperatures will decrease snowpack storage in higher elevation mountains of western North America as precipitation falling as snow declines (Harpold et al, 2012). With temperatures forecasted to increase there is potential for a decrease in Snow Water Equivalent (SWE) and a shorter duration of snow covered season (Dozier, 2004). As a result, water loss will be greater as drier and warmer conditions in these regions will increase evaporative losses in our water storage reservoirs, soils and plants. In addition to the previously mentioned changes, New Mexico specifically, is projected to experience smaller snowpacks, earlier snowmelt, and reduced groundwater recharge (Allen *et al.*, 2005). Water is crucial to New Mexico's growth and economic development and is already generally over

allocated in some of New Mexico's larger river basins, such as the Rio Grande (Allen *et al.*, 2005).

Observations in the coastal ranges of the Cascades and Sierra Nevada mountains have documented declines in Snow Water Equivalent (SWE) and shifts to an earlier onset of melt over the last 50 years (Dozier, 2004). More recently, analysis of US Geological Survey (USGS) stream flow data in Arizona and New Mexico showed that 60% of annual runoff generation can be attributed to snowpack melt (Hawkins et al, 2007), reiterating the importance of mountain snowpacks in the west and southwest.

With many of the fastest growing cities in the US situated in the mountain west regions combined with over allocated water resources, it is vitally important to understand how changes in mountain snowpack depth and distributions could impact the aforementioned communities. Harpold *et al.* (2007) found that decreased duration of snow cover, reduced maximum SWE and shorter melt duration all threaten snowpacks of the arid southwest. To better predict these changes in water production, it is necessary to gain a more detailed knowledge of the snowmelt energy balance of shallow snow as well as quantification of lower elevation snowline energy fluxes (Bales *et al.*, 2006). This research aims to give quantification of energy fluxes on the snowpack across varying gradients and aspects in the Jemez Mountains of New Mexico.

Snowmelt and ablation are driven primarily by energy exchanges at the snow/atmosphere interface, however the role of energy fluxes at the ground/snow interface where shallow transitional snowpacks exist are less understood. A case study in Arizona by Hawkins *et al.* (2007) aimed to investigate how snowpack energy fluxes varied compared to more heavily studied regions with deeper seasonal snowpacks. They found the ground heat flux was far more

significant in the arid mountain location when compared to previous studies in maritime snowpacks of California and high elevation continental snowpacks of Colorado.

In the arid southwest, there has been little research describing the role of ground surface temperature and the ground heat flux on snow processes. Temperature at the snow/soil interface strongly affects physical processes that occur in snow-dominated environments (Tyler *et al.*, 2008). Cooling at the interface of shallow snowpacks allows freezing of the soil and retards infiltration at the beginning of snowmelt (Dunne and Black, 1971), which could affect future runoff and storage for snow dominated mountain regions affected by climate change.

This research aims to improve understanding of the influence of the ground heat flux on snowpack processes through a case study in the Jemez Mountains of north central New Mexico. The study objectives will be met by: (1) compare ground heat flux in the Jemez Mountains to other study areas using the model SNOBAL and determine if 0℃ ground temperatures are a reasonable assumption; (2) compare calculated and modeled ground heat flux values; and (3) determine if near-surface ground temperatures can be used as an indicator of snowpack ripening and snow cover.

1.1 Background

There are a variety of anthropogenic effects inducing climate change that can alter the state of mountain snowpacks. In the mountains of the western US, sharp wet-dry seasonal transitions, complex topographic and landscape patterns, steep gradients in temperature and precipitation with elevation, and high inter-annual variability make hydrologic processes and variations significantly different from lower elevation regions or those that are humid all year (Bales et al, 2006). Bales *et al.* (2006) also noted the spatially fragmented and temporally varying distributions of climate, land cover, geology, and snow both characterize and complicate

the hydrology of the mountain west regions. This has led to a variety of topics being studied in order to begin to grasp the complicated nature of snow ablation processes. Of these, the net radiation flux in a mountain snowpack is noted as one of the most important processes of snowpack ablation that is linked to the water cycle.

1.1.1 Energy Balance of Snowpack

The exchange of energy between the snowpack and its environment ultimately determines the rate of snowpack water losses due to melting and evaporation/sublimation. Energy exchange primarily occurs at the snowpack surface through the exchange of shortwave and longwave radiation and turbulent or convective transfer of latent heat due to vapor exchange and sensible heat due to differences in temperature between the air and snow (DeWalle, 2008).

Small amounts of energy can be added from warm rainfall onto the snow surface as well as ground heat conduction into the base of the snowpack. Changes in snowpack temperature and meltwater infiltration also provide a small amount of internal energy exchange within the snowpack. When the snowpack melts and ripens there is a release of excess energy that may have been stored during the winter. Although there are other small contributors to the snowpack energy balance, in general the net radiation flux is the most important process of the energy budget associated with a snowpack (Marks *et al.*, 1992).

In a seasonal snow cover, snow is thermodynamically unstable, undergoing continuous metamorphism until it melts and becomes runoff during spring (Colbeck, 1982). These metamorphic changes and final melting are driven by temperature and vapor pressure gradients within the snow cover, which are caused by heat exchange at the snow surface and at the snow–soil interface (Male and Granger 1981). Energy exchange to and from the snowpack can be quantified with a mass balance approach using the following equation.

(1)

$$\Delta Q = R_n + H + L_v E + G + M$$

$\Delta Q = Change\ in\ snow\ cover\ energy$
R_n = *net radiation*
$L_v E$ = *Latent heat flux*
H = *Sensible heat flux*
G = *Conductive Ground heat flux*
M = *Advective heat flux*

A negative energy balance (ΔQ) will cool the snow cover, ultimately increasing the cold content of the snowpack, which is the amount of energy required to bring the snowpack to 0℃. A positive energy balance (ΔQ) will add energy to the snowpack, however cannot exceed 0℃ and ensuing melt cannot occur in any significant amounts until the cold content is satisfied. Futhermore, once the snowpack has reached isothermal conditions at 0℃ throughout the height of the snowpack, all positive values of (ΔQ) must result in melt water being generated.

Net radiation (R_n) is the combination of incoming and outgoing shortwave and longwave radiation. Longwave radiation is emitted by any substance above absolute zero in temperature (DeWalle, 2008). During the winter, atmospheric gases, clouds, forest vegetation, rocks, and the snowpack all radiate longwave radiation. Longwave radiation occurs during both day and night which can increase the impact it has on the snowpack.

Sensible heat (H) exchange occurs whenever a temperature difference exists between the atmosphere and the snow surface. The sensible heat exchange can be affected by the magnitude of temperature difference between the air and snow surface, wind speed and surface roughness. During mid winter the snowpack can be warmer than air temperatures resulting in energy losses from the snowpack to the air (DeWalle, 2008).

Latent heat exchange ($L_v E$) occurs from water vapor exchanges between the snowpack and atmosphere from turbulent mixing in the layer of air just above the snow surface. Transfer

of vapor from the snowpack to the atmosphere constitutes a loss of latent heat of vaporization (evaporation) if the snowpack has liquid water present and a loss of latent heat of sublimation if subfreezing temperatures exist (DeWalle, 2008). This process is seen in the semi-arid mountain regions where during cold temperatures in high elevation mountains water vapor is lost from the snowpack. A study in Colorado found that 20% of the snowpack water equivalent was lost due to evaporation and sublimation

Rainfall energy, which is included in the (M) term can provide sensible heat additions from heat being added when warmer rain falls onto cold snow. Rainfall releases its sensible heat and if that is not sufficient enough to warm the snowpack to 0℃, then the rain water would refreeze and a loss of latent heat of fusion would occur. Overall, this energy flux is a very small component to the energy budget.

Other small terms that are not included in equation 1 are internal snowpack energy storage and melt energy. Internal snowpack energy storage can change if there are sensible heat changes from snowpack temperature changes and mass increases from snowfall. An example of this would be if the snow surface thaws and refreezes during night time, there would be an energy deficit created which would need to be satisfied before melt could occur the next day. In the same scenario where the surface layer thawed during the day and began to infiltrate the snowpack, if the water did not refreeze and did not drain from the snowpack, there would be a gain in latent heat of fusion. If that melt water did refreeze within the snowpack there is no net energy gain. If the melt water drains completely from the snowpack you have melt energy loss, which is a loss of latent heat of fusion when liquid water drains from the snowpack (DeWalle, 2008).

According to Sturm (2015), a 50 year assessment of snow hydrology publications appearing in the Water Resources Research Journal, one of the largest research categories at 8% of papers involved research on snow energy balance topics. Through the progression of snow energy balance studies, the focus has been primarily on radiation and turbulent exchanges where models have parameterized the ground heat flux component. Energy balance studies focusing on net radiation and turbulent fluxes have become a primary focus in relation to snowpack melt processes in deep snowpacks. Many studies have essentially ignored G, however have indicated the significance of G during portions of the season. In California, Marks and Dozier (1992) found that radiation provided 66%-90% of the energy for snowmelt with ground heat flux (G) accounting for 1%, producing melt water in midwinter. A study in a high altitude location in Colorado by Cline (1997) found net radiation and turbulent fluxes to account for up to 75% of snowmelt energy over the season and also noted that G was insignificant except during the end of the season when the snowpack was thin.

1.1.2 Ground Heat Flux

Ground heat flux to the base of the snowpack generally represents a very minor energy source for melt (DeWalle, 2008). The small contributing factors of soil heat conduction are associated with the fact that soil is a poor conductor of heat. Heat transfer from soils tend to be small when compared to the seasonal energy balance of the snowpack and can be ignored or greatly simplified (Marks and Dozier, 1992). Temperatures in soils are often fairly low (near 0℃) due to the lack of solar warming beneath deep snowpacks. In regions with deep seasonal snowpacks, heat conducted from the soil can contribute to gradual ripening and slow melting of basal snow layers, however this process usually decreases into spring when the snowpack is

shallow (DeWalle, 2008). When snowpack depth decreases to about 20 to 25cm then transmission of shortwave radiation to the ground has a larger impact on ground heat conduction.

Ground heat flux is largely ignored in the modeling of snowmelt processes particularly among spatially explicit models (Lamontagne, 2009). There are generally simplifications in many of the snowmelt models for ground heat flux because high energy sources like solar radiation, longwave radiation and turbulent heat fluxes are far more dominant on the snowpack (Smith *et al.*, 2008). In locations with cold soils, and thin or transient snowpacks, the ground heat is small due to the lack of opportunities for ground heat to generate snowmelt. In temperate regions where soils freeze irregularly or for limited durations and where deep insulating snowpacks persist, substantial ground heat flux generated snowmelt may occur and may result in substantial snowpack loss over a winter period (Smith *et al.*, 2008).

Various studies have found G to be more important during certain times of the winter or at different stages of melt. This usually occurs early in the season or later when the snow depth is less than 0.5m (Lamantagne, 2009). Contributions of G may also be higher during very cold ambient temperatures creating a temperature gradient over the space of the snowpack. This causes vapor diffusion from the warm ground towards the cold atmosphere conducting heat into the base of the snowpack. Similarly, a study in the prairies of Canada where shallow snowpacks persist showed that G varied diurnally (Granger, 1978). Additionally, a study in Norway showed that between two snow seasons, the deeper snow year reduced heat exchange between the ground and atmosphere by 70% (Boike *et al.*, 2003). Sensoy *et al.* (2006) in a cold and shallow snowpack region in the mountains of Turkey found that modeling the snowpack with the assumption of the ground surface temperature of 0°C was not reasonable due to increased interaction between atmosphere and ground.

Smith *et al.* (2008) found that pre winter conditions were a large determinant of hydrothermal conditions in deep snowpack regions. The comparison of the winters 2007 and 2008 showed two different pre snow weather conditions resulting in different G values during the winter. In 2007, early snowfall preserved a warmer ground surface, thus increasing the temperature gradient between the snow/ground interface. In 2008, a lag in snowpack development allowed ground surfaces to freeze before a seasonal snowpack developed, therefore decreasing the temperature gradient during snowpack development.

Cline (1997), while investigating a high elevation site in Colorado found that net radiation and turbulent heat fluxes accounted for 75% and 25% of the energy generated for snowmelt respectively. This study also found G to be negligible with exception of late season measurements when the snowpack was shallow. In Idaho, a study by Marks *et al.* (2001) found snowmelt to be driven by net radiation and sensible heat, however at their higher ridgeline study site they found G to be much larger due to a shallower snowpack resulting from higher winds redistributing snow and therefore, reducing snow cover. In a mountain area characterized by shallow snow and early meltout, this result shows that the contribution of G may not be very large, however implicates the importance of G in melt generation in shallow snowpacks.

Finally, a study more climatically similar to New Mexico conducted by Hawkins *et al.* (2007) in a mountainous area in central Arizona provides evidence that the nature of snow ablation in the arid climate of the southwestern US may be very different from that in the traditionally studied higher latitude climates. This study examined the differences in the energy budget of more commonly studied mountain snowpack regions. The key differences underlying the study were that most energy balance studies have been conducted in areas of high elevation and seasonally deep snowpacks. In Arizona, the contrast is stark, snow is more transient, often

going through multiple ablation periods and is persistently shallow. This type of climate and snowpack could be an indicator of what the future might look like for a snowpack in New Mexico.

Hawkins *et al.* (2007) found that the contribution from G is increased in this region because of shallower snowpacks, inducing more ground/atmosphere interaction. They also found that the contributions of turbulent fluxes were different with a greater contribution of sensible heat fluxes and a lower contribution of latent heat fluxes. Net radiation in the Arizona study was negative, which was likely due to the solar angle ultimately decreasing shortwave radiation. This study occurred much earlier in the calendar year as snowpack ablation occurs months earlier in Arizona compared to California, for example. The temporal differences indicate why radiation terms are different and highlight the importance of latent heat of sublimation and vaporization from the snowpack in the arid southwest climate. Table 1 shows comparisons of previous study locations and the ground heat flux contribution percentages.

Location	**Elevation (ft)**	**Dates**	**G Flux %**
Happy Jack, AZ	7672	12/31-2/6, 2007	18
Niwot Ridge, CO	11606	4/25-6/6, 1997	3
Emerald Lake, CA	10180	5/1-5/31,1986	1

Table 1 Comparison of ground heat flux percent of radiation balance incident the snopack from selected snow covered mountainous areas (Source: Table manipulated from Hawkins *et al.*, 2007).

As indicated previously, the majority of the research in relation to the energy balance and ablation of mountain snowpacks, particularly in the US, has been conducted in areas with deep seasonal snowpacks and mid latitude high elevation locations. At locations with seasonal snowpacks, warm soils are typically covered by early season snows which are slowly cooled during the course of the winter. In the spring, zenith angles are low inducing rapid snowpack melt. Soil temperatures are often near 0°C as snowpack ripening is beginning to occur. As ripening nears, melt water begins percolating vertically through the snowpack and removes the

remaining temperature gradient thus reducing the G flux (Lamontagne, 2009). Alternatively, at low latitude, low elevation, and more arid regions such as New Mexico, shallow transient snowpacks dominate and temporal changes in the energy balance occur.

1.1.3 Snowpack Ripening

Snowpack temperatures can vary seasonally and daily as a result of complex processes of energy transfer within the snowpack (DeWalle, 2008). Depending on meteorological and snowpack characteristics, near surface temperatures of the snowpack can be subfreezing due to interaction with the cold atmosphere, however at the base of the snowpack can be near 0°C in midwinter due to soil heat conduction. In spring, when air temperatures are warmer and snowpacks are becoming shallower, the snowpack is warmed to 0°C spanning the height of the snowpack thus becoming isothermal.

The process involved for the snowpack to reach isothermal conditions is complex and has many contributing factors. The process can start when water is generated at (or just below) the snow surface by melting snow where liquid water percolates into the snowpack and first contacts below 0°C snow grains. These grains achieve a more rounded shape and the larger grains grow in size as the smaller grains lose mass to them (Wakahama, 1968). The resulting difference in grain-size and configuration combined with pre-existing variations in microscale snowpack structure (e.g. wind crusts, buried sun crusts, different snow grains, buried surface hoar, irregular microtopography) lead to a non-uniform distribution of liquid water, which enhances differences in rates of metamorphism and consequent grain size (Colbeck, 1978). When the snow is at 0°C, liquid water is retained by capillary pressure in the pore spaces between the snow grains. More water is held in smaller pore spaces with fine grains than in snow consisting of larger grains resulting in large pore spaces. In a case where smaller grained snow layers overlie larger grained

snow layers, water will accumulate in the upper layer until the pressure difference between the layers is relieved and water can then flow into the lower layer (Wankiewicz, 1979).

Warming of snowpacks from the surface enhances melt water infiltration where liquid water eventually refreezes when encountering the colder grains, which in turn warms those same grains from latent heat exchange. Flow fingers or preferential flow paths can then develop which aid the transport of water through cold snow until it reaches a layer that is less permeable. This causes the water that is infiltrating the snowpack to spread and then refreeze creating an ice layer. Ice layers that form will have an effect on the overall ripening process. These ice layers can also form at the soil/snow interface if the soil is below 0°C and has limited permeability (Woo, 1981). Once the snowpack is warmed to 0°C and liquid water holding capacities are satisfied, the snowpack can begin to release water from its base (DeWalle, 2008).

Being able to determine when the snowpack is ripe is important because it can help signal the output phase of the snowpack when water runoff is being generated. Furthermore, having the ability to determine when the snow has disappeared from a slope is important in order to track the spatial extent of snow cover, which could aid in model and forecast accuracy. Schmid *et al.* (2012) cite two distinct points in snowmelt processes that can be recognized to help to quantify patterns of snowmelt. The first characteristic is the melt out date, when the snow cover is depleted and no melt water is further released allowing the ground surface temperature to warm above 0°C. The ripening date is the other characteristic that can be determined when the ground surface temperature is at 0°C from melt water percolation. The sharp change in the amplitude of the daily ground surface temperature can be used to detect the first and last day of snow on the ground (Zhang, 2005) and also indicate snowpack ripening (Lundquist, 2008).

1.1.4 Shortwave Solar Radiation Penetration of Snowpacks

The net flux of shortwave radiation typically represents the major source of energy for snowmelt and can be quantified as the sum of incoming and outgoing shortwave radiation fluxes. As solar radiation is emitted from the sun it is absorbed, refracted, and reflected by constituents in the atmosphere, which can diffuse its impact on the snow surface. The Zenith angle of the sun plays a large role in the intensity of solar radiation into and out of the snowpack. The intensity of solar radiation varies temporally and with latitude, which ultimately changes the zenith angle in relation to the snowpack surface seen in Figure 1. On clear days about 80% of incoming shortwave radiation occurs as direct beam and 20% occurs as diffuse shortwave radiation (DeWalle, 2008).

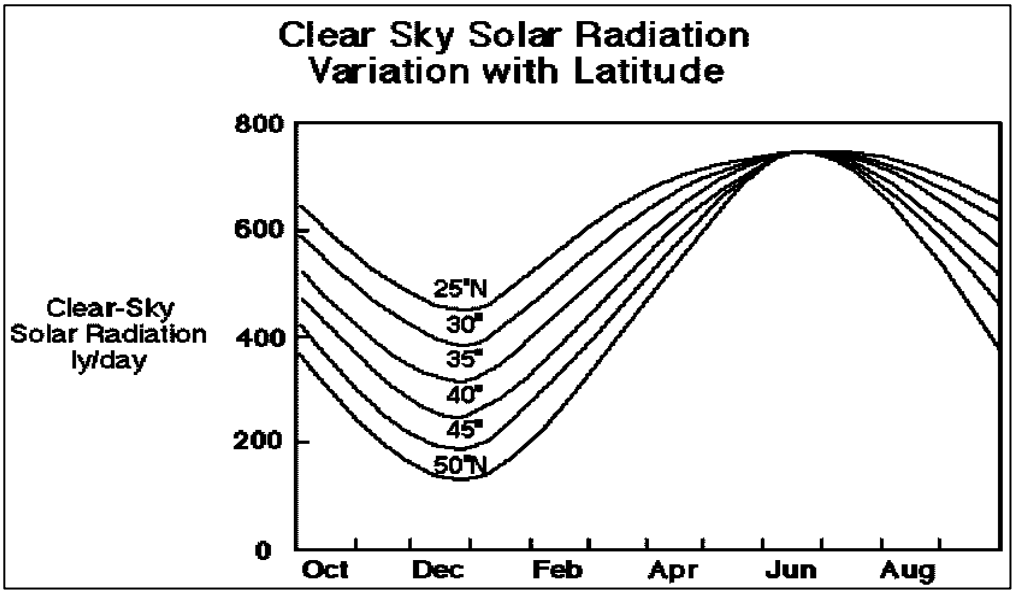

Figure 1. Variation of clear sky solar radiation with time of year and latitude. (Source: Anderson, 2006).

As solar radiation is emitted onto the snow surface, it can be transmitted, absorbed, or reflected by the snowpack. When solar radiation strikes the snow surface, up to 90% is reflected back into space when the snow cover is new dry snow (McClung, 2006). The portion of solar

radiation that is not reflected can then penetrate into the snowpack, however the intensity will decrease exponentially with depth as seen in Figure 4.

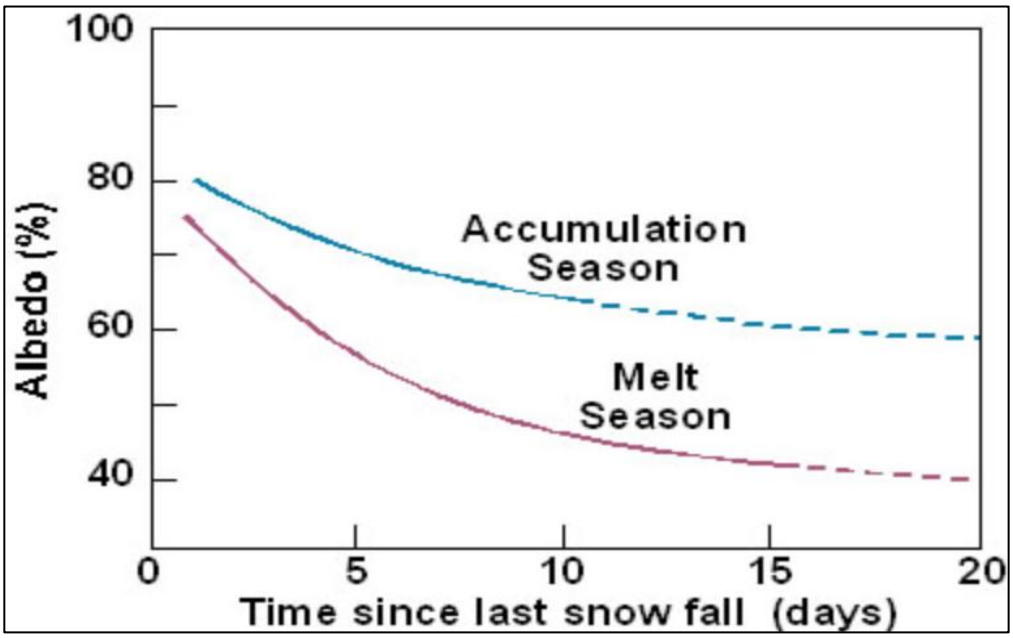

Figure 2. Albedo and Time since last snowfall are compared by time of snow season. Accumulation season is before peak depth occurs and melt season is during warmer and longer days after peak depth has occurred. (Source: UCAR, 2007)

Factors that influence the fate of solar radiation incident to the snowpack are surface albedo, grain size, density and moisture content. Snowpack albedos are expressed as a percent of reflectivity and can range from .95 (95%) for newly fallen snow to .4 for more dense dirty snow. The snow surface albedo changes over time as density changes and follows a decay curve dependent upon how long the snow has been on the ground seen in Figure 2. As the transition from low density new snow goes through the settlement process resulting in higher density snow, the albedo will decrease ultimately increasing the ability to transmit solar radiation. In conjunction with this, as settlement occurs resulting in increased grain to grain contact the snowpacks ability to transmit solar radiation will also increase through conduction.

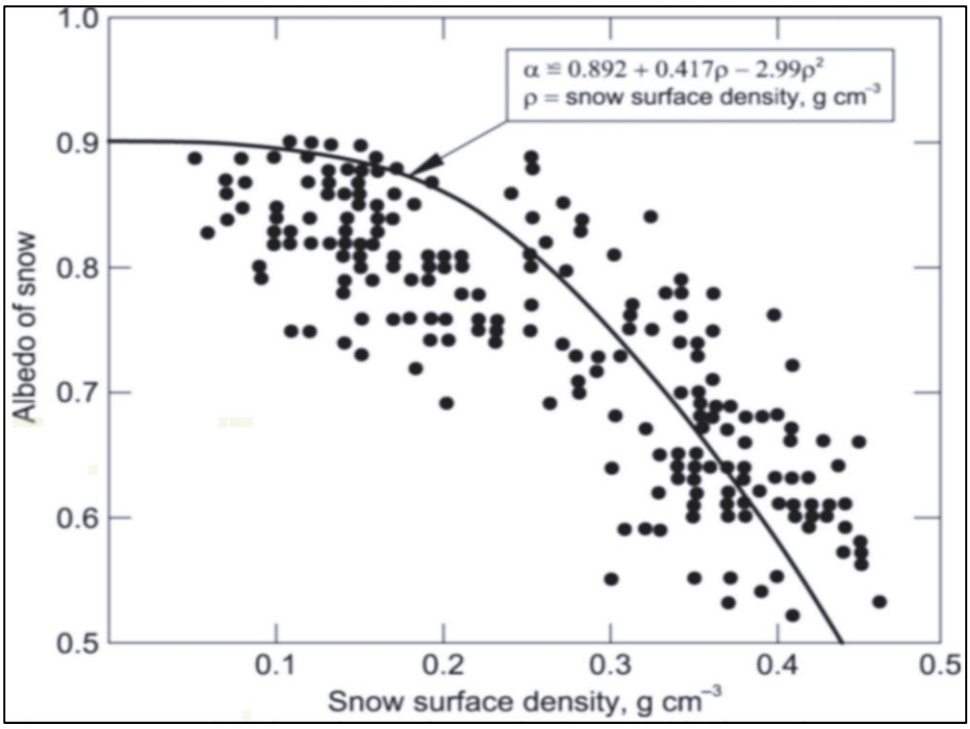

Figure 3. Snowpack Albedo as a function of snow density (Source: DeWalle, 2008).

Warming can occur of underlying objects that are buried by the snowpack such as rocks and soil which will enhance melting and through conduction and a decreasing snow surface albedo as these objects are shallow enough to receive solar radiation. Visible light penetrates shallow snow providing energy to heat the underlying soil resulting in increased heat conduction to the snow (Baker *et al.* 1991).

For freshly fallen fine grained snow the distance of solar radiation penetrated into the snowpack is as small as a few centimeters (McClung, 2006). For dense, dry snow conditions with densities of 100 kg/m^{-3} solar radiation penetration is around 10cm into the snowpack and less than 10% of the solar radiation remains deeper than 10cm (McClung, 2006). Penetration of solar radiation is generally deeper in snowpacks that consists of large grained snow. Figure 4 depicts the type of snow grain in relation to the light extinction curve for each. For a black surface, 40% of incoming solar will reach the surface below 1cm of snow and 3%-4% will reach

the surface below 10 cm of snow (Baker *et al.*, 1991). For solar energy levels sufficient to raise soil temperatures, 10 cm is the accepted maximum depth (Baker *et al.* 1991).

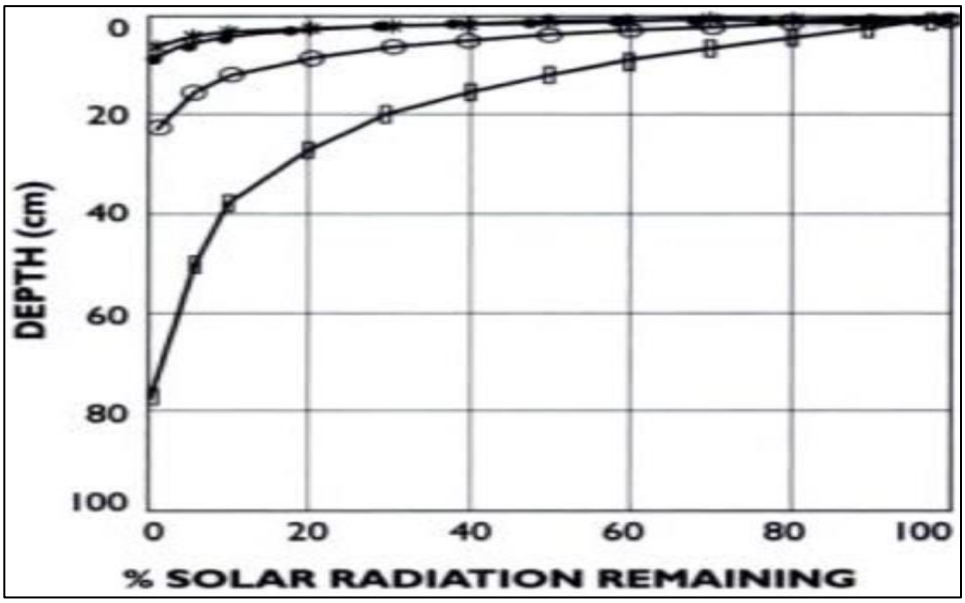

Figure 4. Penetration of Shortwave Radiation in the snow cover and percent of solar radiation remaining at that depth. Different snow grain types are compared. ∗ = newly fallen snow, · = fine grained snow, ∘ = coarse grained snow, ■ = glacier ice. (Source: McClung, 2006)

In deeper snowpacks where the overlying snow effectively insulates the ground, solar radiation will not have in impact on ground temperatures until it is reduced to about 20-25cm in depth (DeWalle, 2008). According to Baker et al (1991) if the snow albedo is above 70% then dark plants and soil surfaces will not affect snow surface albedo.

During the ripening process the snowpack contains more water and is denser, therefore, transmits solar radiation more effectively. Feedback loops exist in this process as the surface albedo declines, there is more radiation being absorbed by the snowpack increasing snowpack settlement. As settlement increases grain to grain contact increases resulting in greater heat conduction between grains. This then results in increasing melt resulting in larger grains. As melting increases, shallower snow results giving more efficient solar radiation transmission

through the snowpack to the underlying surface. In the semi-arid mountains of New Mexico, snowpacks in some areas typically remain shallow enough in which solar radiation could potentially penetrate to the underlying ground. Also, the metamorphic processes occurring in the warm semi-arid climate may also induce deeper solar penetration into the snowpack throughout the winter

2. STUDY SITE

2.1.1 Site Location

The Valles Caldera National Preserve (VCNP) is 30km southwest of Los Alamos, NM in the Jemez Mountains situated in north central New Mexico. This site was chosen for its location, as snowmelt runoff feeds into Albuquerque and Santa Fe, two of the largest cities in New Mexico. The landscape is unique in that a series of volcanic eruptions left behind volcanic cones and domes and a large crater shaped landscape in the center. The highest peak in the VCNP is Redondo Peak at 11,254ft, which is located 2 miles south of the study area. The surrounding mountains near the study area are around 10,00ft and valley elevations are generally around 8400ft. The study site is located in the Alamo Creek Watershed on the west side of the Preserve just north of Redondo Peak. Figure 5 shows the Alamo Creek Watershed and the position within the VCNP. It also shows the location of the data collection points.

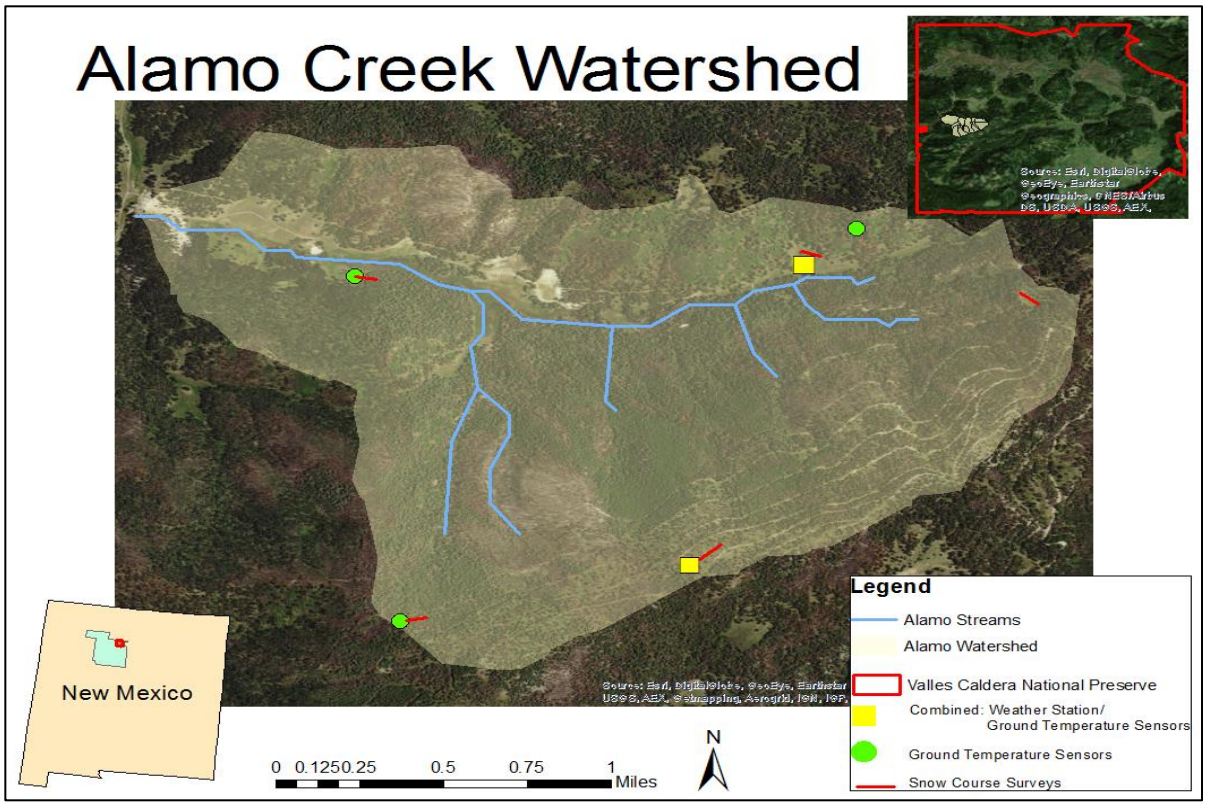

Figure 5. Alamo Creek Watershed with locations of measurements as well as measurement types.

2.1.2 Climate

The regional climate in the Jemez Mountains is considered semi-arid continental, which is characterized by low snowfall and cold temperatures. The majority of precipitation (60%) comes from summer monsoon events and winter precipitation typically falls as snow (Muldavin, 2003). The Jemez Mountains generally experience shallow seasonal snowpacks on north facing aspects and intermittent snowpacks on south facing aspects. During the winter months temperatures average in the mid 20's°F on Redondo Peak (11,254ft). In the winter, the valley bottoms are characterized by large diurnal temperature fluctuations. When evaluating weather station data from Redondo Peak, temperatures in the winter months are as high as 60°F and as low as -20°F in the valley bottoms. Temperature inversions are common in these valleys during the winter months.

The Quemazon SNOTEL station located near Los Alamos, NM is situated at 9500ft in elevation about 20 miles east of the study site. This weather station shows a mean annual precipitation value of 48cm of which 35% falls as snow between October and April, with average temperatures of 9℃ from 1980 to 2011 (Harpold *et al.*, 2014). The average snow depth at Quemazon SNOTEL calculated from available data spanning 2001 to 2014 is 17.60in.

2.1.3 Snow Season 2015/2016

The 2015/2016 snow season was characterized by a strong El Nino – Southern Oscillation (ENSO) pattern in which forecasters were calling "Godzilla". Typically, an ENSO pattern will result in above normal precipitation for the New Mexico. This assumption held true for a portion of the season with early winter season snowfall resulting in accumulations in the Alamo Creek Watershed as early as Oct 21. Snow continued to accumulate through November and December 2015. As of January 1, 2016, snowpacks around the state were 141 percent of normal (Romero, 2016). In February the precipitation events diminished with one significant event on Februrary 20th. The weather in February was characterized with high pressure and the snowpack was reduced to 80 percent of normal. Precipitation in March was non existent and snowpacks declined quickly with warm temperatures. The snowpack in Alamo Creek Watershed melted in early March to early April depending on the aspect and elevation.

2.1.4 Soils

Within the VCNP there are about 20 different soil types depending on the locations that have been mapped by the Natural Resources Conservation Service. The soils fall within two large groups, either forest or grassland. The forest soils are primarily mountain soils and are derived from volcanic rocks and gravel along with some windblown deposition (Muldavin, 2003). The mountain soils tend to have very rocky/gravel characteristics with loam textures in

between. The grassland soils consist mostly of Mollisols that have developed in the volcanic alluvium of the alluvial fans or in recent water deposited sediments of the valley bottoms (Muldavin, 2003). Mullisols are characterized by thick dark fertile soils from long term organic materials being added. (McDaniel, n.d.). According to the mapped soils by the NRCS, the valley bottom of Alamo Creek Watershed consists of Palon cobbly sandy loam on 15 to 35 percent slopes. The higher elevation site of Alamo Creek Watershed consists of Calaveras Rubble on 35 to 60 percent slopes (Muldavin, 2003). The lower weather station consists of Cosey-Jarmillo (304) and the upper weather station consists of Calaveras Rubble (83).

Soil Properties within the Alamo Creek Watershed							
Soil Description	**Soil #**	**Bulk Density (g/cm3**	**Hydraulic Conductivity µm/s**	**Clay %**	**Sand%**	**Silt %**	**Organic Matter %**
Palon Cobbly	72	1.47	36.5	10	66.9	23.1	2.59
Calaveras Rubble	83	1.66	124.76	12	64.8	23.2	0.28
Cosey-Jarmillo	304	1.4	16.3	24.5	37	38.5	0.87

Table 2. Soil Characteristics within the Alamo Creek Watershed. Palon Cobbly at upper elevation near ridge tops. Calaveras Rubble and Cosey Jarmillo located in the valley bottoms. (Source: Natural Resources Conservation Service, n.d.)

3. METHODS

3.1.1 Instrumentation

Two Cabell Scientific weather stations were deployed within the Alamo Creek Watershed equipped to measure precipitation, temperature, barometric pressure, net radiation, wind speed and direction, below ground moisture and temperature, and snow height.

Measurements were taken every 15 minutes and stored by a data logger. The weather stations were up and running by mid December 2015. The locations for the two weather stations were chosen to capture climatic conditions on top and on the bottom of the watershed with a high north facing location of 9,800ft and a slightly south facing aspect in the valley bottom at 8,600ft.

Image 1. Upper Weather Station at 9800'

3.1.2 Snow Profiles

Two snow study plots were established on a north and south facing aspect near the weather stations in order to best correlate weather and snowpack conditions. Study plots are used to observe and record parameters for long-term records (Greene *et al.*, 2010). These sites were chosen to minimize contamination of the observations by external forces such as wind, solar radiation, slope angle, and human activity.

Snow profiles were conducted monthly on each aspect to track changes in snowpack conditions. Profiles were excavated to the ground and each subsequent pit was dug at least one meter away from the previous pit. The data collected during snow profile sampling were the height of snow (HS), snowpack temperatures at 10cm vertical increments, layer boundaries, layer densities, layer grain form, and layer grain size. Snow profile methods were followed by the guidelines established in the Snow, Weather, and Avalanche Observation Guidelines (SWAG) (Green *et al.*, 2010).

Temperature profiles are useful for determining the metamorphic trend the snowpack is going through. By tracking temperature changes throughout the snowpack the temperature gradient can be observed, which will help indicate the vapor flux direction. Grain size and form of each layer was collected to identify if the snowpack is sintering or faceting, either reducing or increasing the snowpack ability to conduct heat. Densities of each layer were collected to identify water content within the snowpack. Snowpack height was measured to help determine the overall snow water equivalent (SWE) which will be used to calibrate SNOBAL point models.

Image 2. Author performing layer density measurements during a snow profile on 2/12. Additional data collected during the snow profile were layer characteristics, grain types and size, and temperatures

3.1.3 Snow Course Surveys

Snow surveys are conducted in order to obtain information about water supply, aid in forecasting flood and droughts, and other water resource studies. The data collected from snow surveys provides regional information of water resources for power generation, irrigation, industry, fisheries and wildlife, and recreation (Ministry of Environment, 1981).

Five snow course survey sites were established throughout the Alamo Creek Watershed in order to characterize the snowpack depth and SWE at different elevations and aspects throughout the accumulation and ablation season. One snow course was set up at the mid elevation site at 9400ft where temperature sensors were also buried. Another snow course site was setup at 9800ft near the upper weather station and a third site was setup at 9000ft to capture

snowpack data near the valley bottom. Each snow course survey was 100m long with depth measurements taken every meter and SWE measurements every 10m.

Snow course surveys were completed bi-weekly starting in December. A federal snow sampling tube was used to measure the depth of snow and the length of the snow core contained in the tube. The tube was then weighed and the tube weight was subtracted to determine the SWE.

3.1.4 Ground Temperature Data Logger Placement

The resolution at which one should measure snowpack variability depends on the problem being addressed. Snow depth variability has been measured with various methods including extensive depth probe sampling (Elder *et al.,* 1991), Lidar (Deems *et al.* 2006) 10 ibuttons (small temperature sensors) distributed randomly in $10m^2$ areas (Schmid *et al.* 2012) and 2-3 temperature sensors in a 100m area (Lundquist *et al.* 2008). In the mountains of the western US, snow depth varies at hillslope scales (1-100m) because of wind and avalanches (Elder *et al.,* 1991) and additionally vary from differences in vegetation cover (Anderson *et al.*, 2004). In the Jemez Mountains, observations also suggest that snow distributions vary significantly by aspect and elevation. At scales over 100m, slope, elevation, net radiation, precipitation amount, and air temperature become more important (Erxleben *et al.*, 2002).

Based on the techniques used by Schmid *et al.* (2012) and the recommendations from Lundquist *et al.* (2008) a combination of their methods were chosen for data collection in the Alamo Creek Watershed. Five footprints consisting of four HOBO temperature sensors were deployed throughout the watershed to capture near surface ground temperatures in order to infer snowpack ripening, ground heat flux, snow onset, and day of snow disappearance. All footprints

are represented by variations in burial depths for each sensor ranging from 2cm to 10cm. The spacing between sensors was 10m placed vertically across gradients.

Three footprints were deployed on the north facing aspects spanning the horizontal and vertical distance of the Alamo Creek Watershed. The upper elevation footprint is at 9800ft at 350°NW, 9400ft at 352°NW, and 8600ft at 340°NW. Two footprints were deployed on south facing aspects at 8600ft at 180 °S and at 9070ft at 180 °S. Each location was chosen to minimize the effects of wind redistribution of snow in order to reduce the number of sensors needed per Lundquist *et al.* (2008) recommendations. Footprints were placed in open areas to reduce the effects of vegetation radiation fluxes incident to the snowpack. Furthermore, energy fluxes in openings are also more easily interpreted under clear sky conditions and are also recommended for baseline snow conditions per (McClung, 2006).

3.1.5 Ground Heat Flux Calculations

The ground heat flux, or the amount of heat flowing upwards from the interior of the earth and into the base of the snowpack, was calculated using measurements from buried ground temperature sensors. The amount of energy received at the base of the snowpack is dependent on the thermal conductivity of the underlying soils and can be calculated with the one-dimensional steady state heat flow in a homogenous layer using the following equation:

$$G = k \frac{\partial T}{\partial z} \quad (2)$$

where:

G = Soil heat conduction, $W\,m^{-2}$
k = thermal conductivity of soils, $W\,m^{-1}\,K^{-1}$
z = soil depth, m
T = temperature °K

In order to calculate the ground heat flux, soil thermal conductivity needs to be determined. The method chosen to calculate the thermal conductivity of soils was with Kersten's method (Farouki, 1981). Kersten's method gives the thermal conductivity in terms of its moisture content and its dry bulk density as soil conductivity can change with moisture content. The equation for unfrozen soils was chosen based on the soil characteristics that exist in the Alamo Creek Watershed. Below is the empirical equation used to calculate the thermal conductivity of unfrozen soils:

(3) $$K_g = 0.1442(.9\,Log(w) - .2)10^{.6243\gamma d}$$

where:

K_g = *thermal conductivity of soils,* $W\,m^{-1}\,K^{-1}$
w = *moisture content of soil %*
γd = *dry density of soils* $g\,cm^{-3}$

The value obtained from Kersten's Method was then used to calculate the Effective Thermal Conductivity (K_{eg}). The thermal conductivity of soils is corrected because the air fraction of the snowpack is always at saturation, and the air fraction of soil is usually near saturation (Marks et al., 1992). Therefore, vapor diffusion is estimated as a function of snow temperature, soil temperature and air pressure. Applying these adjustments results in the following equation:

(4) $$K_{eg} = K_g + (L_v D_e q_g)$$

where:

K_{eg} = *effective thermal conductivity of soils,* $W\,m^{-1}\,K^{-1}$
K_g = *thermal conductivity of soils,* $W\,m^{-1}\,K^{-1}$
$L_v = latent\ heat\ of\ fusion$ $(2.834\ x\ 10^6, m^2\ s^{-2})$
D_e = *diffusion coefficient (1.37 x* 10^{-5}, $m^2\ s^{-1}$)
q_g = *specific humidity (4.847 x* 10^{-3})

To obtain the diffusion coefficient in equation 4, equation 5 was used

(5) $$D_e = D \frac{P_0}{P_a} \left[\frac{T_{s1}}{T_{melt}}\right]^{nt}$$

where:

$D_e = diffusion\ coefficient$
D = diffusion coefficient for vapor in soil at sea level $(10^{-5}, m^2\ s^{-1})$
P_0 *= sea level pressure 101 KPa*
P_a *= pressure at study site 73.59 KPa*
T_{s1} *= temperature snow ground interface, K*
T_{melt} *= melt temperature, K*
nt = temperature exponent

The next calculation needed in order to calculate the ground heat flux was the effective thermal conductivity of snow (K_{es}). The thermal conductivity (K_s) of snow is a function of density. Snow densities of each snowpack layer were measured monthly during snow profile measurements. Measured density values ranged from .22-.35 $g\ cm^{-3}$. The equation used to calculate the thermal conductivity of the snow layer above the ground was developed by Sturm et al., 1997 and is as follow:

(6) $$K_s = 1.38 - 1.01\rho + 3.233\rho^2$$

where:

$K_s = snow\ thermal\ conductivty, W\ m^{-1}\ K^{-1}$
$\rho = density\ of\ lower\ snow\ layer, g\ cm^{-3}$

Similar to the adjustments made for the effective soil thermal conductivity, there were physically based adjustments made to calculate effective thermal conductivity with the following equation

(7) $$K_{es} = K_s + (L_v D_e q_s)$$

where:

K_{es} *= effective thermal conductivity of snow,* $W\ m^{-1}\ K^{-1}$
K_s *= snow thermal conductivity,* $W\ m^{-1}\ K^{-1}$
$L_v = latent\ heat\ of\ fusion$ $(2.834\ x\ 10^6, m^2\ s^{-2})$
D_e *= diffusion coefficient (1.37 x* 10^{-5}, $m^2\ s^{-1}$)
q_s *= specific humidity (4.847 x* 10^{-3})

Soil and snow temperatures near their interface are typically very similar, therefore the calculation of heat transfer between them is based on the assumption that the two represent a homogenous layer in contact with each other (Marks et al., 1992). The final equation for the ground heat flux (G) then becomes:

(8)

$$G = \frac{2K_{es}K_{eg}(T_g - T_s)}{K_{eg}z_s + K_{es}z_g}$$

where:

G = ground heat flux, $W\,m^{-2}$
K_{es} = adjusted thermal conductivity of snow, $W\,m^{-1}\,K^{-1}$
K_{eg} = adjusted thermal conductivity of soils, $W\,m^{-1}\,K^{-1}$
T_g = soil temperature measurement, K
T_s = temperature measurement in snow, K
z_s = height of snow measurement up from base of snowpack, m
z_g = depth of measurement under ground, m

Equation 8 was also compared to values produced by equation 9. The main difference in equations is that equation 8 accounts for the snow characteristics and equation 9 calculates G values based solely on soil conditions. The equation used to calculate the ground heat flux is below:

(9)

$$G = K_g \frac{T_g - T_{sb}}{z_2 - z_1}$$

where:

G = Soil heat conduction, $W\,m^{-2}$
K_g = thermal conductivity of soils, $W\,m^{-1}\,K^{-1}$
z = soil depth, m
T_g = soil temperature, K
T_{sb} = temperature at the base of the snowpack z_1, K

3.1.6 Modeling the Snowpack

The snow cover energy and mass balance model (SNOBAL) represents the physics of the snow cover energy balance and snowmelt, and has been shown to accurately represent both the development and ablation of the snow cover during a wide range of climate characteristics, snow cover conditions, and geographic locations (Marks *et al.*, 1998). Figure 6 is a conceptual diagram of the SNOBAL model. SNOBAL is a point model, which was then developed into a distributed model version called ISNOBAL.

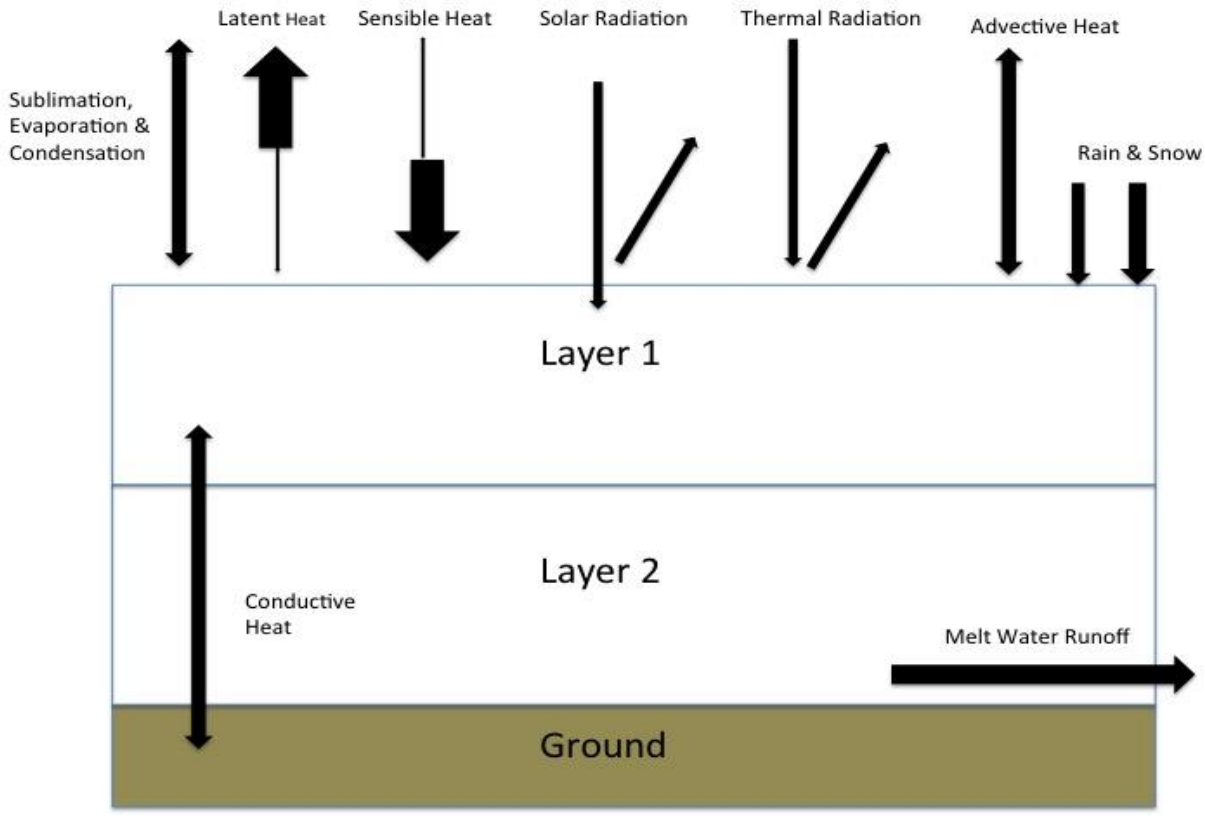

Figure 6. Conceptual diagram of the SNOBAL energy balance snowmelt runoff model, showing the energy and mass fluxes considered and calculated at a single grid point, and the layering structure of the simulated snow cover. (Source: Recreated from Marks, 1999).

The SNOBAL model is initiated by using measurements of snow depth, density, temperature and SWE. Following these initial inputs are independent inputs consisting of net

solar radiation, precipitation mass, temperature, and estimated density in order to calculate the energy, mass balance, and runoff from the snow cover (Marks *et al.*, 1998). The model generates predictions for snowmelt in two snow cover layers, runoff from the base of the snowpack, and adjusts the snow cover mass, thickness, and thermal properties. Lastly, SNOBAL calculates the snowpack height at each time step.

State and forcing variables are required by the model in order to generate model runs and forecasts. The state variables are input as initial conditions consisting of snow depth, snow density, snow surface temperature, average snow cover temperature, and average SWE and are then predicted as the model runs. The forcing variables are used by the model to predict the changes in the state variables and are input at each time step of the model run. The forcing variables consist of net solar radiation, incoming thermal radiation, air temperature, vapor pressure, wind speed, and soil temperature. The parameters and variable descriptions are listed as follows:

Initial Condition Variables

$Z_s = total\ snowcover\ depth\ (m)$
$\rho = average\ snowcover\ density\ (kg\ m^{-3})$
$T_{s,0} = snow\ surface\ temperature$ (℃)
$T_s = average\ snowcover\ temperature$ (℃)
$W_c = percentage\ of\ liquid\ water\ in\ snowpack$

Forcing Variables

I_{lw}= incoming thermal (long-wave) radiation (W m^{-2})
$T_a = air\ temperature$ (℃)
$e_a = vapor\ pressure\ (Pa)$
u = wind speed ($m\ s^{-1}$)
$T_g = soil\ temperature$ (℃)
$S_n = net\ solar\ radiation$ (W m^{-2})

The SNOBAL model outputs generated from recorded meteorological and snowpack data relating to energy and mass flux are the averages for all energy balance terms and snow conditions and are as follows:

Energy and Mass Flux Output
$R_n = average\ net\ all\ wave\ radiation\ (W\ m^{-2})$
$H = average\ sensible\ heat\ transfer\ (W\ m^{-2})$
$L_vE = average\ latent\ heat\ exchange\ (W\ m^{-2})$
$G = average\ snow/soil\ heat\ exchange\ (W\ m^{-2})$
$H = average\ adevected\ heat\ from\ precipitatoin\ (W\ m^{-2})$
$\Delta Q\ = average\ sum\ of\ energy\ balance\ terms\ for\ snow\ cover\ (W\ m^{-2})$
$E_s = total\ evaporation\ (kg\ m^{-2})$
$q_{melt} = total\ snowmelt\ (kg\ m^{-2})$
$q_{out} = total\ runoff\ \ (kg\ m^{-2})$
$cc_s = snow\ cover\ cold\ content\ \ (kg\ m^{-2})$

Snow Conditions Output
$z_s = predicted\ snow\ cover\ thickness\ (m)$
$\rho = predicted\ average\ snow\ density\ (kg\ m^{-3})$
$m_s = predicted\ snow\ cover\ mass\ (kg\ m^{-2})$
$w_s = predicted\ liquid\ water\ in\ snow\ cover\ (kg\ m^{-2})$
$T_{s0} = predicted\ temperature\ of\ surface\ layer$ (℃)
$T_{s1} = predicted\ temperature\ of\ lower\ layer$ (℃)
$T_s = predicted\ temperature\ of\ snowcover$ (℃)
$z_{sJ} = predicted\ thickness\ of\ lower\ layer\ (m)$
$w_{sat} = predicted\ percent\ of\ liquid\ water\ saturation\ of\ snow\ cover$

3.1.7 Model Calibration

Data processing for SNOBAL inputs required calibration and corrections to some of the parameters that were measured. The first category of data that needed to be input was climate data consisting of shortwave and longwave radiation, air temperature, soil temperature, wind speed, and vapor pressure. Vapor pressure was calculated with dew point temperature air temperature and relative humidity with the following equations

(10)

$$T_d = T - \frac{100 - RH}{5}$$

where:

$T_d = dew\ point\ temperature$ (K)
T = temperature (K)
RH = Relative Humidity

(11)

$$e = 6.11 * (10^{\frac{7.5*T_d}{237.3+T_d}})$$

where:

e = vapor pressure (hpa)
T_d *= Dew Point Temperature (°K*)

The second input category was precipitation record, which included total precipitation mass, percent of precipitation mass that was snow, density of snowfall, and average precipitation temperature. Because of the error associated with capturing snowfall, precipitation totals were corrected for false recordings in the rain gauge by evaluating wind speed and relative humidity. Precipitation amounts were further corrected for under catch by precipitation gauges by adding 25% to each precipitation event per findings from Hodgkinson et al. (2004). Density of snowfall was input according to new snowfall density charts from DeWalle et al. (2008) since onsite new snow densities were not measured at the time of snowfall. The range used was 60 to 250 kg m^{-2}. Average precipitation temperature was assumed to be the dew point temperature.

The third input category were measurement heights, which included the height of wind speed measurement, height of temperature measurement, roughness length, and the depth of soil temperature measurement. The height of the temperature and wind speed measurements were set as 3m. The soil temperature measurement was at 2cm below ground. The roughness length is the height at which the wind speed becomes zero and was set the .001m according to Marks et. al (1998).

The final input category were snow properties, consisting of snow cover depth, average snowcover density, active snow layer temperature, average snowcover temperature, and percent of liquid H2O. The snow cover depth was initiated at .75m based on field measurements and the day the model run started. The active snow layer temperature and average snow temperature were based on field measurements during snow profile assessments of -6°C and -3.33°C respectively. The snow cover density was initiated at 265.37 kg m^{-3} according to field measurements. The percent of liquid H2O was set according to recommended default by Marks et al (1998).

The model was run for the time period starting on January 18, 2016 ending the day the snow disappeared on April 7. Model calibration was accomplished by using total snow depth as the calibration point. SNOBAL was not very sensitive to precipitation events while going through the calibration. For SNOBAL to better represent the actual measured snowpack depth, the density of new snow was increased for some of the precipitation time steps. The density was increased from 100 kg m^{-2} to 250 kg m^{-2}. This adjustment helped increase the precipitation events enough to better represent measured snow depths. Also, being sure to add the assumed 25% under catch by precipitation gauges and distributing precipitation events over more time steps helped calibration.

Once precipitation events were calibrated, the ground temperature depth and temperature measurements were adjusted to test the sensitivity of these changes to model results. Changing the depth from .5m to .02m had little effect on the rate of melt. Changes in the temperatures had more effect, but still minimal

In order to increase the melt rate during the later part of the season the solar radiation numbers were adjusted. One justification for raising these numbers was the location of the net

radiometer sensor as it was located in a tree shadow during the times of greatest incoming solar radiation. Therefore raising this number was reasonable given that it was likely under measuring during the melt season. Solar radiation at the upper site had diurnal fluctuations ranging from 0 to 400 W m^{-2} in January and February and 0 to 650 W m^{-2} during late March and early April.

Further justification for raising the solar radiation numbers were to allow for the effects of decreasing snowpack albedo. As the snowpack warms and begins to go through near surface melt freeze cycles, moisture content and snow grain growth will decrease snow pack albedo and enhance melt rates. Slightly raising the solar radiation numbers allowed for this effect.

4. RESULTS

4.1.1 Snow Course Measurements

Measuring snow depth in five locations throughout the Alamo Creek Watershed allowed the inspection of snow depth distribution throughout the course of the winter. Figure 7 shows each snow course site illustrating the average depth differences between each site as well as the duration of snow cover throughout the season.

The Upper North snow course accumulated the most amount of snow and took the longest to melt out. Higher accumulation was expected due to effects of orographics in mountain terrain. The meadow site, although lower than the Mid North site accumulated more snow due to the lack of canopy cover intercepting snowfall. The Low South snow course accumulated the least amount of snow and melted out the fastest.

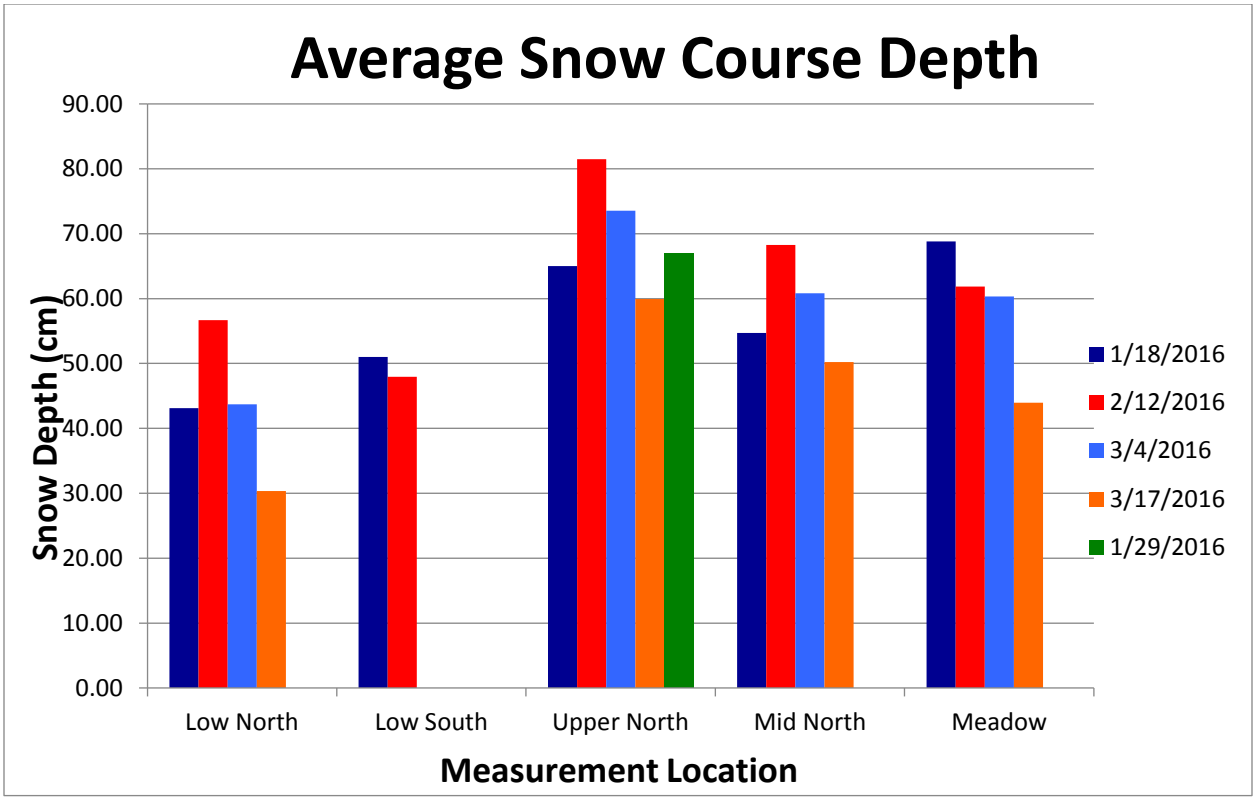

Figure 7. Average Snow Depth per Snow Course Location and date the measurement was taken

The variability in snow distribution was apparent through measurements of snow depth throughout the season. Figure 8 shows the variability in distribution per snow course site. The Low South and the Meadow sites were located in open areas without forest canopies. This allowed for more uniform accumulation and less variability in depth distribution at these sites.

The two sites that showed the highest variability in snow depth distribution were the Low North and the Mid North snow course sites. These two sites went through mixed forest terrain where tree densities varied over space. The variability resulted from areas where there were pockets of open terrain through the forest canopy. The forest canopy limited through fall, resulting in shallower snowpacks in these areas and deeper snowpacks in pockets of open terrain. This observation is important if considering how changes to forest canopy structure can alter snow accumulation.

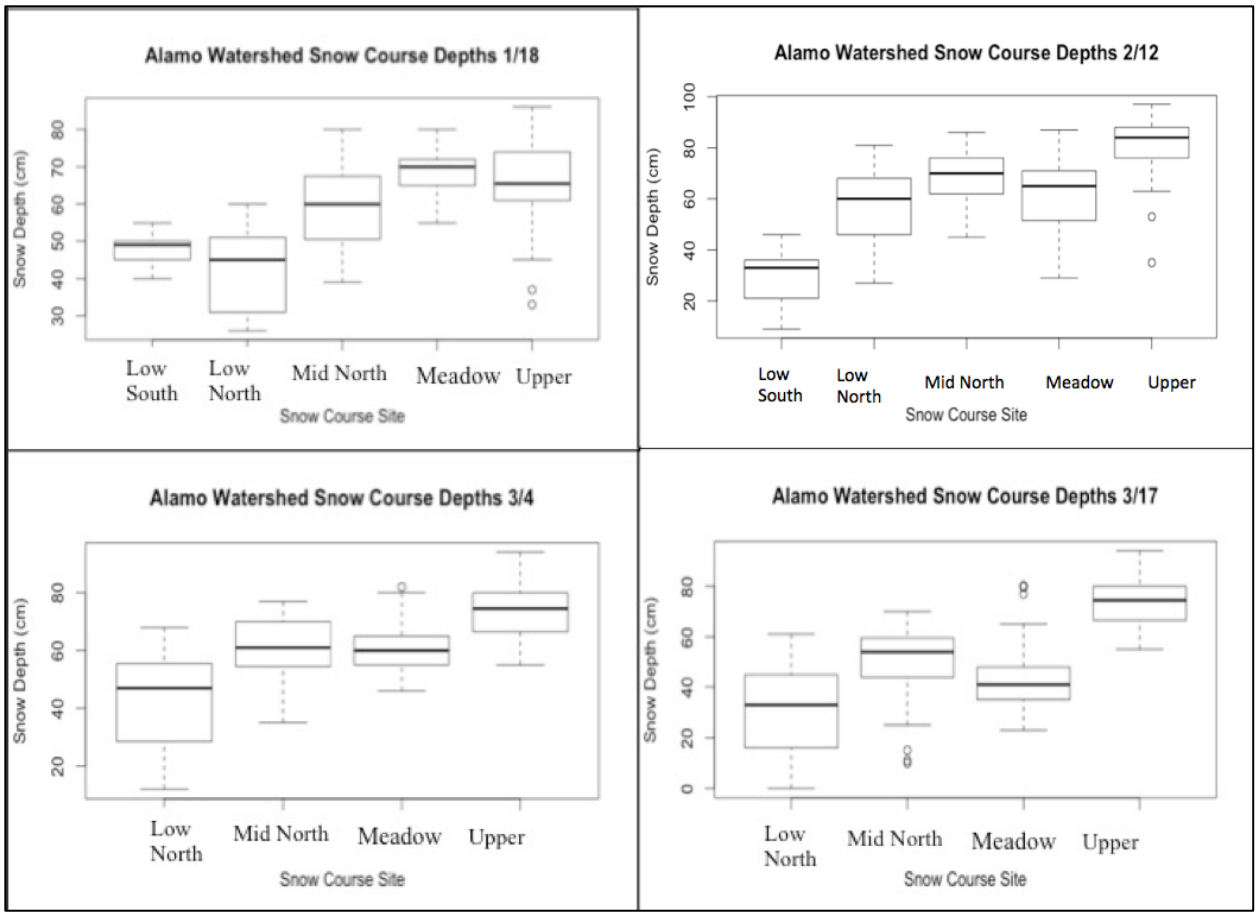

Figure 8. Snow depth variability amongst the different snow course sites based on the day measured. The larger the box the more variability in depth along this snow course transect. Top of box is third quartile (Q3), bottom of box is first quartile (Q1). Dark line through box is median value. Whiskers extend to the highest and lowest values within the upper limit (Q3 + 1.5(Q3-Q1) and the lower limit Q1-1.5(Q3-Q1). Dots are outliers above or below the limits.

Snow Water Equivalent in Figure 9 was greatest at the Upper North site due to the largest amount of snow accumulation. The Low South site had the lowest amount of SWE as a result of the lowest snow accumulation out of all sites. The Meadow snow course generally had the lowest density of sites given the lack of canopy cover. The lack of canopy cover allows for longwave radiative heat loss. This provides conditions suitable for latent heat of sublimation resulting in water vapor loss and a reduction in SWE from this site.

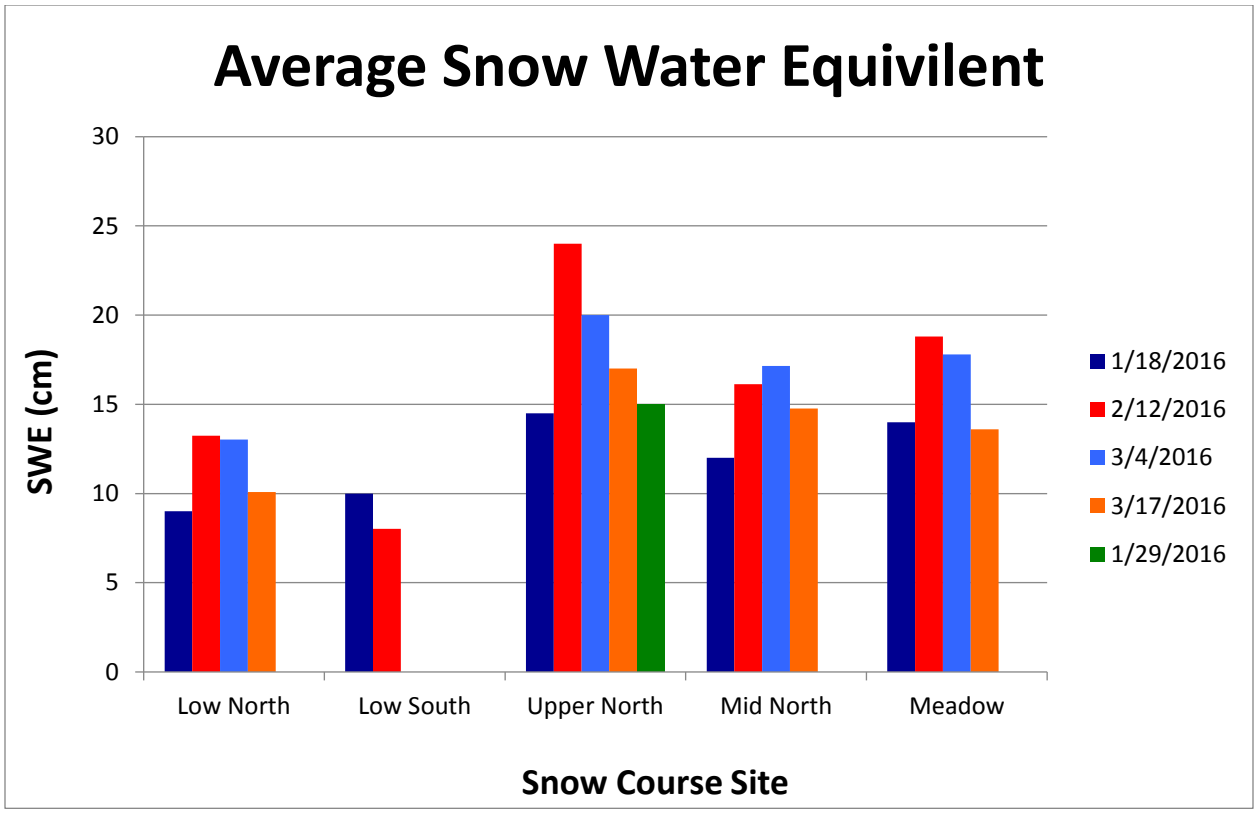

Figure 9. Average Snow Water Equivalent per Snow Course Site and date of measurement

4.1.2 Ground Temperature Measurements

Ground temperature sensor data was plotted to inspect trends and variability. Figure 10 shows the Low Weather Station footprint with four temperatures plotted through the winter season. It is apparent when an insulating snow cover was established due to the lack of diurnal temperature fluctuations noted by the flattening lines in the middle of the time series. The average snowpack depth at the lower weather station reached about 51cm. This depth of snow was enough to insulate ground temperatures from diurnal temperature fluctuations.

The Figure 10 footprint shows an early season snow event in late November as indicated by the dampening of diurnal temperature fluctuations by all temperature sensors. The return of diurnal temperature fluctuations through late November and mid December show that there was no snow present. In mid December a seasonal snowpack was established which is indicated by

the flattening of the temperature profiles. On March 1, the return of these temperature fluctuations indicated the melt of snow from the surface.

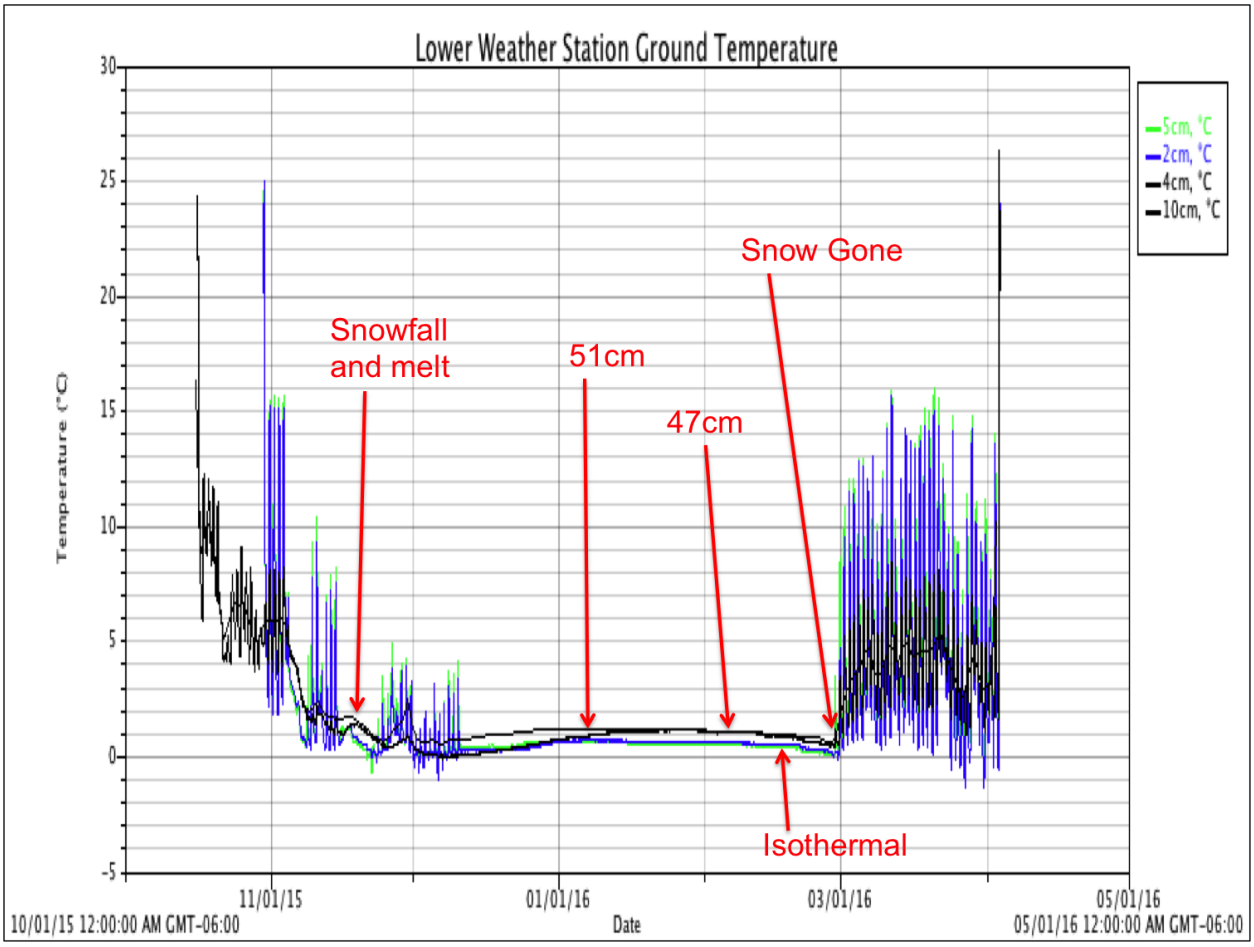

Figure 10. Ground Temperatures at Low Weather Station Footprint. This graph also shows average snow depths from snow course measurements on 1/18 and 2/12. There was snowfall in mid November which then melted and is indicated by the dampening of diurnal temperature fluctuations. On 2/19 the snowpack was isothermal or ripe, meeting the conditions for melt water to trickle out the bottom of the snowpack.

Figure 11 zooms into the period of the snow covered season at the lower weather station. The ground temperatures were warmer than expected, remaining above 0°C. Temperatures deeper underground remained warmer throughout the course of the snow covered season as indicated in Figure 11 comparing 10cm to 2cm depths.

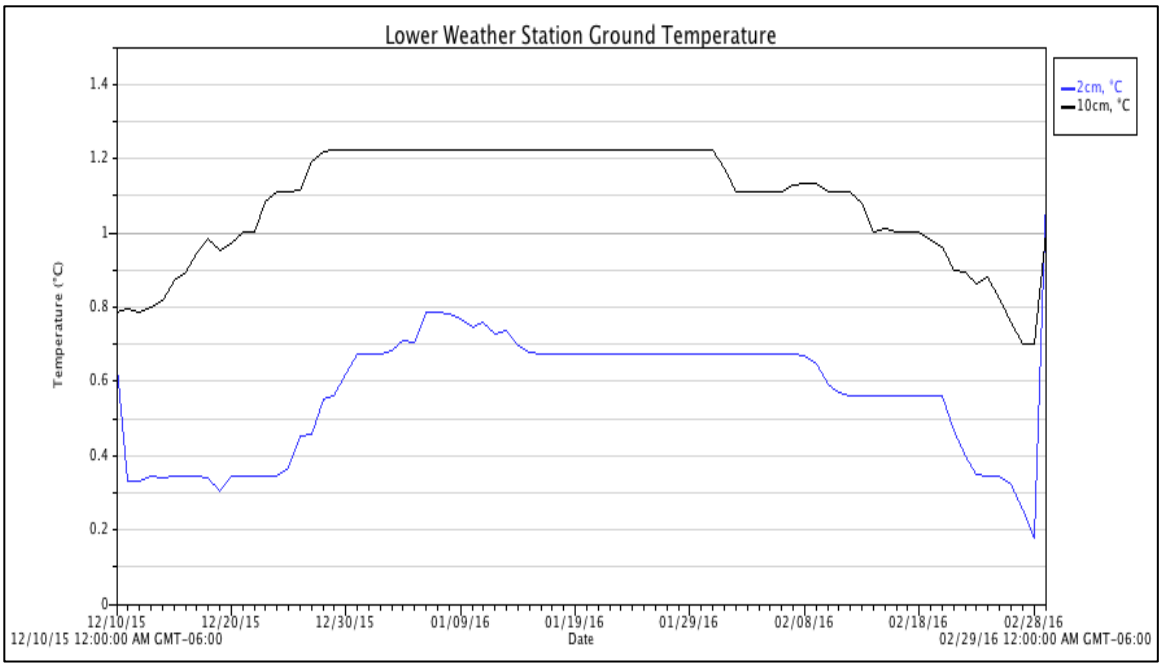

Figure 11. Ground Temperatures at Low Weather Station during the period of snow cover. The two temperature depths plotted are 2cm and 10cm under the snow surface.

Figure 12 is the upper weather station temperature profiles and depths through the season.

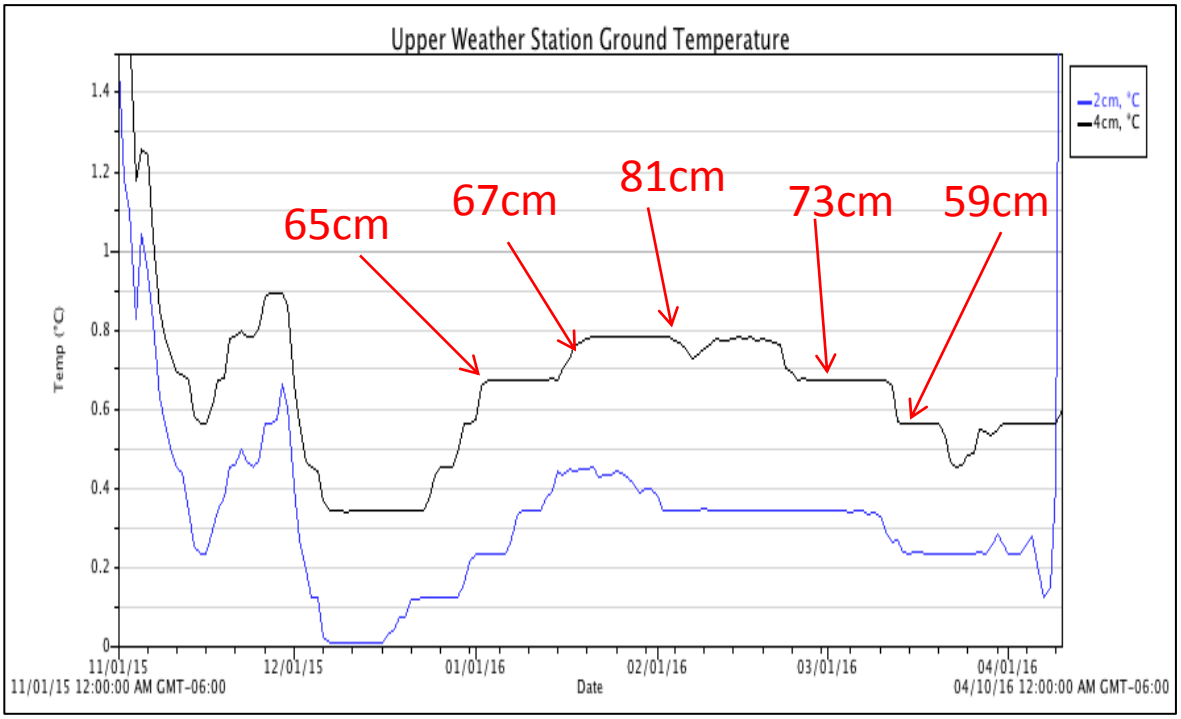

Figure 12. Snow Covered Ground Temperatures at Upper Weather Station with snow depth markings which correlate to the date in which the depth was measured. The red labels indicate the depth of the snowpack in relation to the ground temperatures which are indicated by the time series line.

4.1.3 Calculated Ground Heat Flux

The changes in temperatures through vertical distance indicated in Figures 11 and 12 were used to calculate the ground heat flux. Soils data was obtained through the Natural Resources Conservation Service (NRCS) STATSGO2 database. The ground heat fluxes were calculated at each weather station site for specific dates where ground temperatures and the temperature near the base of the snowpack were recorded during snow profile data collection.

At the lower weather station where soils consisted of Cosey-Jarmillo (fine silty soil) and the upper weather station where the soils were Calaveras Rubble (sand/silt), the ground heat flux was calculated. First K_g was calculated at the lower and upper weather stations using a dry bulk density of 1.36 g cm^{-3} and 1.48 g cm^{-3} respectively derived from NRCS data and moisture content percent, which was measured by weather station instrumentation. The density was held constant throughout the calculation period, however the moisture content was adjusted based on measured data at the lower weather station.

Table 3 shows the measured and derived values that were used to calculate G with equation 9. At the Upper Weather Station the moisture content was constant because no melt had occurred at this location on these dates. The value used for the upper weather station for moisture content was 18% based on STATSGO2 soils data because the soil moisture sensor was not working at the upper weather station. The factors that impacted the amount of G flux into the snowpack were changes in the ground temperature and the temperatures at the base of the snowpack. The ground temperature and temperature at the base of the snowpack were likely changing as a result of the snowpack depth decreasing and moisture from the snowpack penetrating the ground surface.

Date	Avg Moisture %	G (W/m2)	kg	Tg (K)	Tsbase (K)	z2 (m)	z1 (m)
Upper Weather Station							
1/18/16	18	42.24	1.14	273.39	272.65	0.02	0
2/12/16	18	48.12	1.14	273.49	272.65	0.02	0
3/17/16	18	41.78	1.14	273.38	272.65	0.02	0
Lower Weather Station							
1/18/16	36.7	74.5	1.23	273.86	272.65	0.02	0
1/29/16	36.7	75.70	1.23	273.88	272.65	0.02	0
2/12/16	40.5	35.74	1.27	273.71	273.15	0.02	0

Table 3. Ground Heat Flux Calculations based on measured and derived inputs using equation 9

In comparison to the calculated G flux values from equation 9, Table 4 shows the G flux values calculated using equation 8. The assumptions behind equation 8 were discussed in the methods section. One of the main differences in equation 8 is that it includes snow properties. The results indicated that treating the soil/snow as homogenous will decrease the G flux value when compared to equation 9.

Date	Location	Soil Thermal Conductivity (W/m K)	Snow Thermal Conductivity (W/m K)	G (W/m2)
1/18/16	Low wx	1.42	0.21	19.07
1/29/16	Low wx	1.42	0.21	11.76
2/12/16	Low wx	1.46	0.32	11.02
1/18/16	Upper wx	1.33	0.24	10.31
2/12/16	Upper wx	1.33	0.23	10.47
3/17/16	Upper wx	1.33	0.22	9.472

Table 4. Adjusted G Flux Values based on locations of upper and lower weather stations using equation 8, soil and snow thermal conductivities were inputs into equation 8.

4.1.4 Model Results

The SNOBAL model results for snow depth are shown in Figure 13. The green line is the modeled snow depth starting on 1/18 and melting on 4/7 with no precipitation adjustment. Each additional lines are modeled results with precipitation adjustments initially to account for under catch of precipitation gauges as previously noted starting at 25%. This was then increased to in order to test the sensitivity to these adjustments.

The red dots are measured snow depths along the upper weather station snow course site. Snow course measurements were taken on 1/18, 1/29, 2/12, 3/4, and 3/17. The modeled snow depth falls within the actual measured data on each date. Increases along each line are precipitation events that occurred on 1/20 and 2/1. Precipitation events essentially stopped in February and early March as the second half of the 2015/16 winter season was characterized by sustained high pressure.

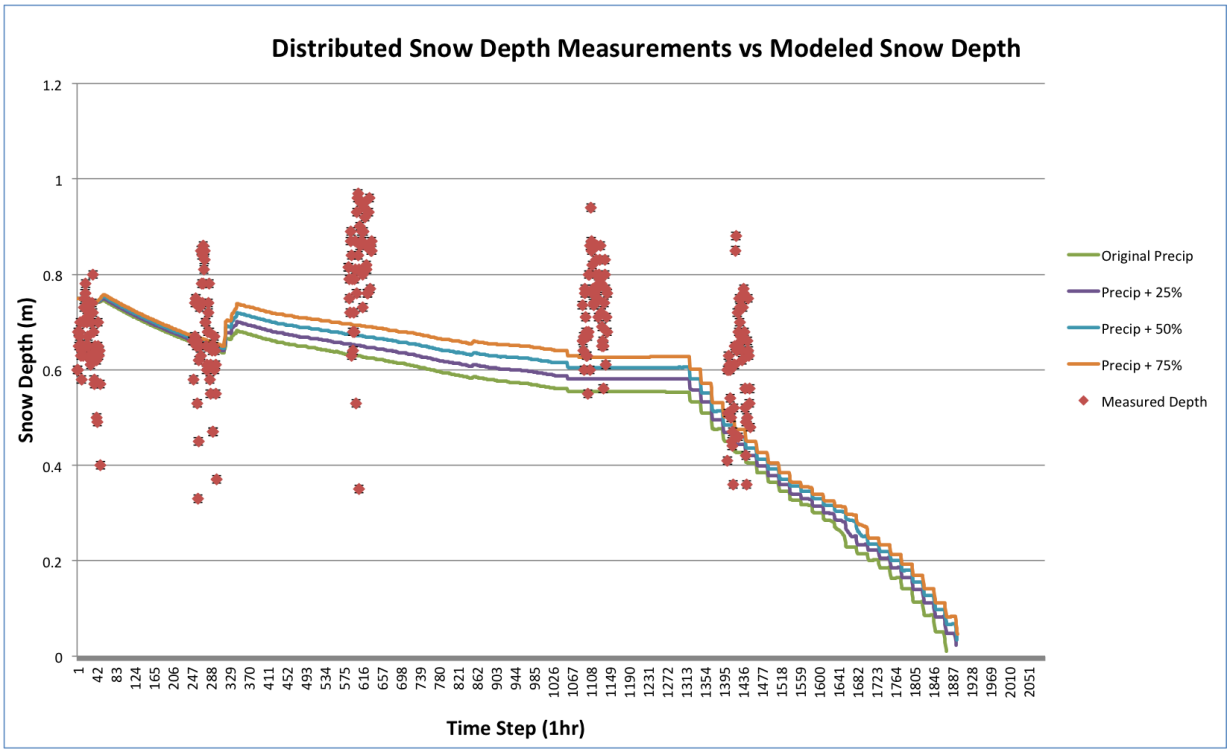

Figure 13. Modeled Snow Depth vs Measured Snow Depth (Timestep: 0 = 1/18, 1000 = 2/19, 1921 = 4/7). The model was initiated on 1/18/16 correlating to the first snow course measurement at this site. The red dots are snow course measurements at the upper weather station. Colored lines indicate percent precipitation adjustments from recorded measurements resulting in snow depth model output.

After SNOBAL was calibrated for snow depth and length of snow season, the ground heat flux was compared to calculated values from point measurements obtained throughout the winter season. Figure 15 shows the modeled ground heat flux compared to two different calculation methods. The green markers in Figure 15 did not correlate with the model runs and on all dates were roughly 30 W m^{-2} higher.

The red markers in Figure 15 represent the method for calculating the G flux using equation 8. The values for this method matched the modeled G values well. Calculated G values only occurred on three dates when measured field data allowed for these calculations. There were no snowpack measurements collected after 3/17.

During mid-season when ground temperatures were warmest the calculated G fluxes were the highest as the warmer ground temperature created the highest temperature gradient between cold snow and warm ground. The modeled G values showed similar results when compared to measured/calculated data. However, the most drastic changes in the G flux occurred later in the season after 3/17. This is when melt at the upper weather station really started to occur as noted by the snow profile on 3/17 where the top 10cm (layer 89-80) consisted of melt/freeze grains shown in Figure 14.

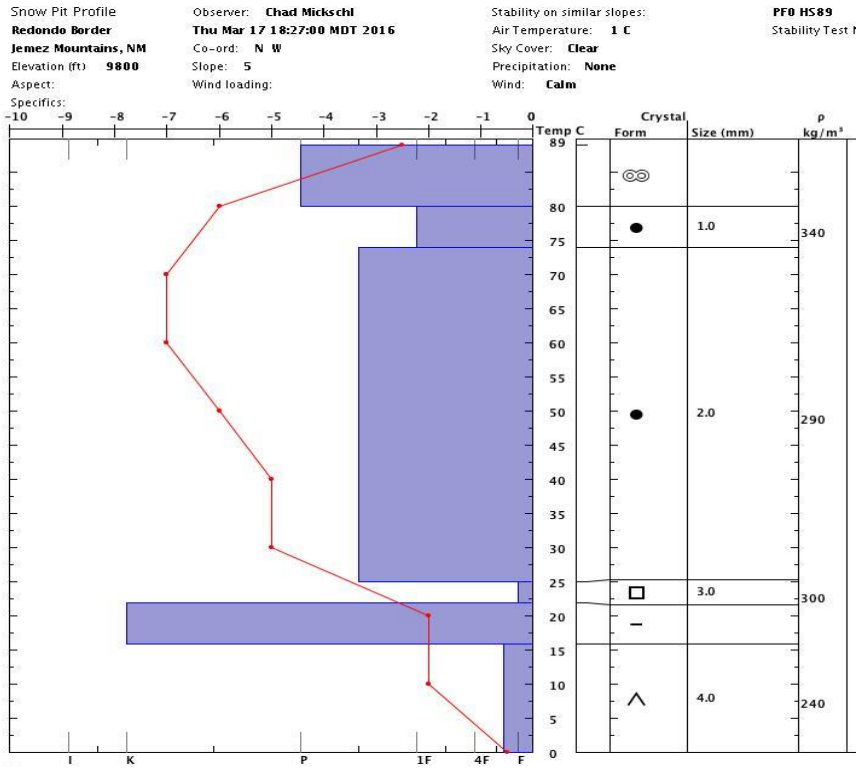

Figure 14. Upper Weather Station Snow Profile on 3/17. The top layer consists of melt/freeze grains indicating the start of the melt/freeze cycle.

The G flux increases significantly during the last week of March when solar radiation values begin to increase. Increased solar radiation is likely penetrating the snowpack, warming ground temperatures near the surface and increasing the G flux. These slight increases are seen in Figure 12 in Late March. This is consistent with literature that cites an increased transmission

of shortwave radiation to the ground occurs when the snowpack is 25cm or less, which will increase the ground heat conduction. On April 1, there is a significant drop in the G flux value as indicated in Figure 15. This drop correlates with overcast sky cover and a precipitation event ultimately decreasing solar radiation and the G flux.

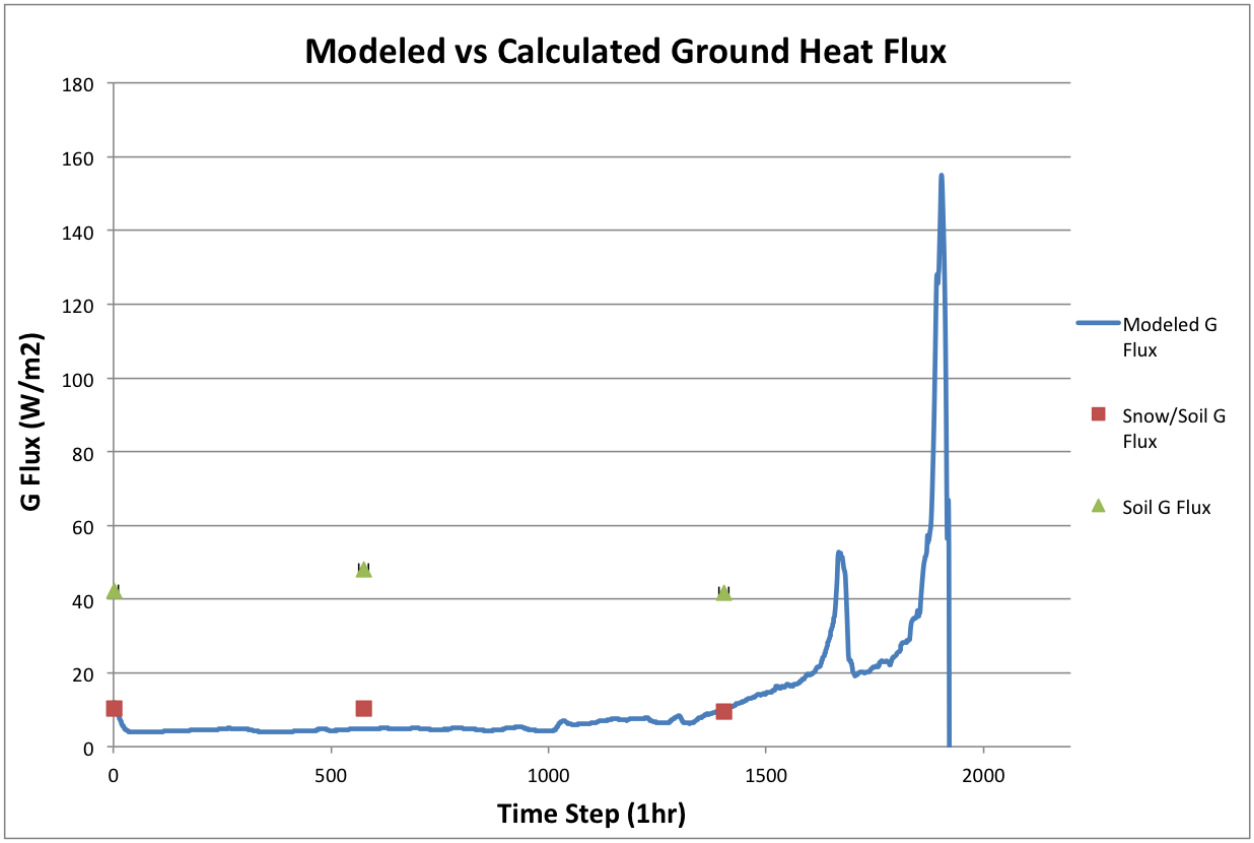

Figure 15. Smoothed Modeled vs Calculated Ground Heat Flux (Timestep: 0 = 1/18, 1000 = 2/19, 1921 = 4/7)

After April 1, ablation of the snowpack goes quickly and disappears by April 7. The melt rate as indicated by the increasing slope on Figure 13 increased due to a combined increase in solar radiation and G flux values. The increase in snowmelt also correlates with the loss of the lower layer of the snowpack in SNOBAL. Once the lower layer is melted on April 1, only the top active layer is left in the model consisting of 25cm. The snowpack is ablating from the top and bottom due to increased solar and G fluxes.

4.1.5 Energy Exchange

Referring back to equation 1, the net energy balance results from SNOBAL are shown below in Table 5. As expected, the colder and shorter days during January and February allow for a net loss of energy (ΔQ) from the snowpack. Net gains of energy (ΔQ) to the snowpack occurred in March and April. April showed a larger increase in (ΔQ) gains when solar radiation as well as G fluxes increased.

The net radiation model output combines short and long wave radiation. January and February shows a net radiation loss from the snow cover and a net radiation gain during March and April as days become longer and the sun is higher in the sky. Sensible heat has a larger effect on the snow cover than latent heat and combining the two shows net turbulent heat gains in all months aside from April. Advection is a minimal input to the snow cover throughout the winter season similar to other studies in other climate regions.

Average Radiation per Month						
	Net Radiation	H	LE	G	M	(ΔQ)
January	-32.80	21.52	-0.12	5.03	1.39	-4.98
February	-19.70	14.28	-0.10	4.61	0.46	-0.45
March	0.86	8.78	-6.70	13.25	0.00	16.19
April	30.01	5.22	-5.90	47.22	0.00	76.56

Table 5. Average per month change in snow cover energy in W m^{-2}

The G flux is small during the colder months, however increases significantly during the ripening and melt season of the snowpack. Judging by near surface ground temperatures, the

snowpack at this upper weather station was likely ripe the last week in March. By the first week in April the snowpack was shallow enough where solar radiation was able to increase the G flux values. The maximum modeled G flux per month is shown in Table 6.

	Max G Flux (W/m2)
January	15
February	6.9
March	111.5
April	208.6

Table 6. Max G value per month

Ground temperatures and different resulting G flux values were an important aspect to look at during this research. Under typical snowpack modeling scenarios the ground temperatures are assumed 0℃. Three different modeling scenarios were ran with different ground temperature regimes to see how the G flux varies. In Figure 16 the three modeling results are shown. The "0℃" scenario is where the ground temperature was assumed 0℃ throughout the snow covered season. G Flux values are the lowest under this scenario. The "0℃" scenario did not result in the snowpack melting by the end of the snow covered season of April 7. The snow does not melt under this scenario by April 7 and the model stops with .15m of snow left on the ground.

The "adjusted" scenario in green is where ground temperatures were changed to achieve melt by the end of the snow covered season. Ground temperatures in the beginning of the season were set colder than recorded temperatures to check for G flux sensitivity. The colder temperatures resulted in a slower melt rate and originally a snowpack that did not melt by the end of the season. The temperatures were then adjusted to .7 and .9℃ toward the end of the

season to achieve the appropriate melt date. The temperatures were then increased to test the assumption that ground temperatures should have increased with more solar radiation.

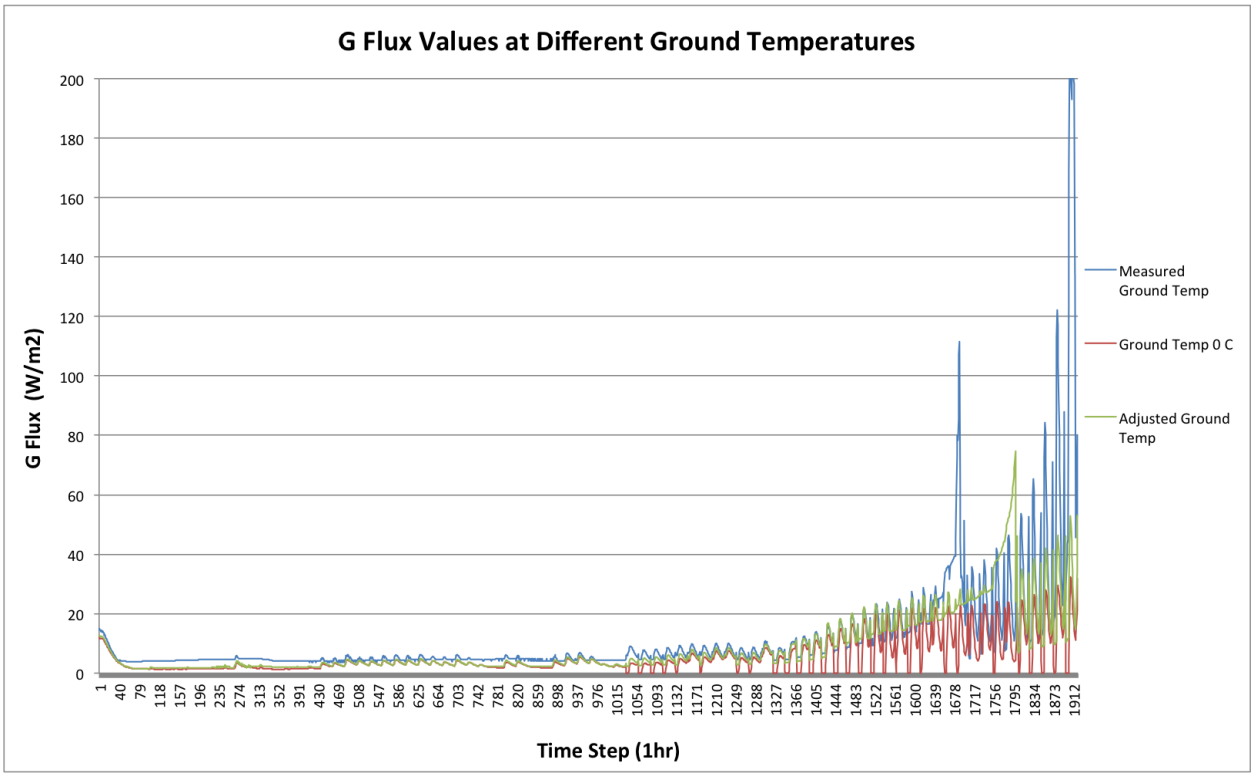

Figure 16. Modeled G Flux with varying ground temperatures (Timestep: 0 = 1/18, 1000 = 2/19, 1921 = 4/7)

The third "measured" scenario in blue was using the recorded ground temperatures. The ground temperatures were slightly positive all winter and at its warmest (.78℃) during the deepest snow cover in mid February. The variations in the G flux scenarios shows that the G flux is greater than the typically assumed 0℃ ground temperature. Figure 17 shows mid season averaged daily G flux values. The G flux values are relatively low, however increase slightly once a seasonal snowpack is established. The "measured" scenario does provide a higher flux into the base of the snowpack than the "0℃".

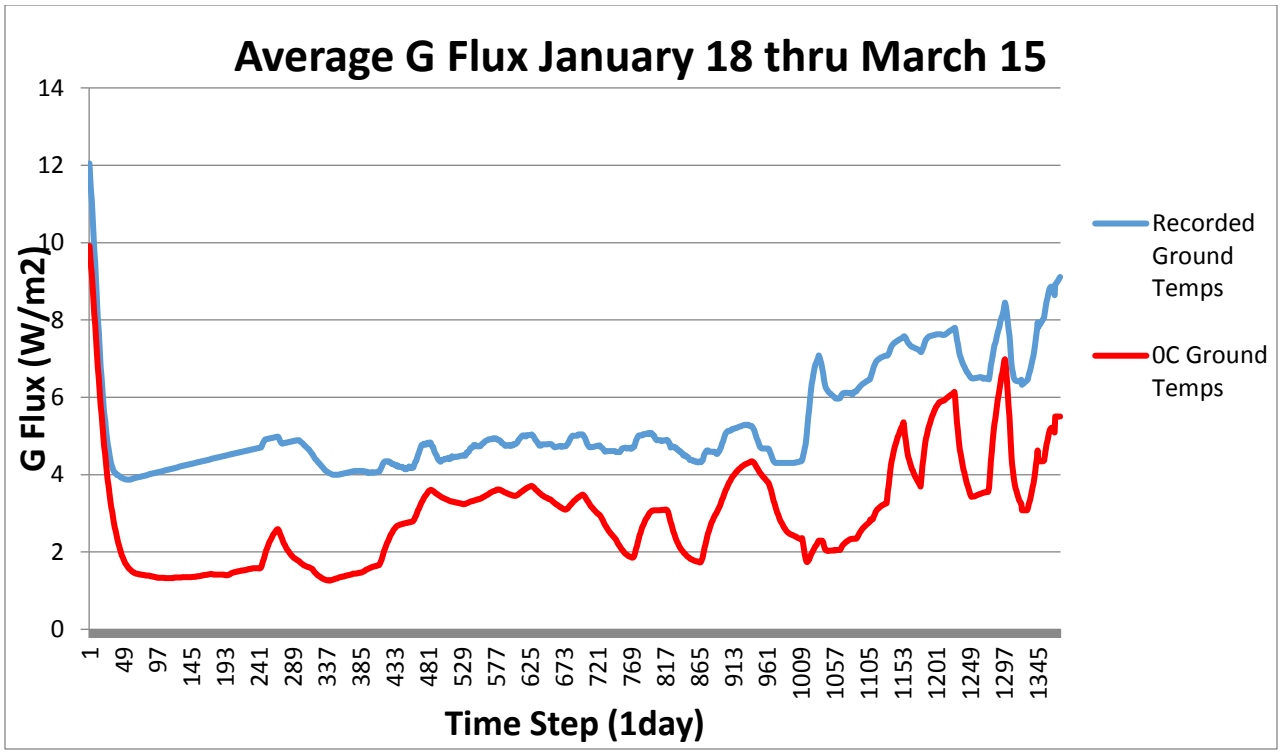

Figure 17. Average Modeled G Flux (Timestep: 0 = 1/18, 1000 = 2/19) This graph shows a snapshot of the first half of the winter and the G flux value of the model scenario

As previously mentioned the difference in fluxes becomes more significant during the end of the season during the melt period. The average G flux for the "0℃" scenario was 6.3 W m^{-2} with a maximum of 46.6 W m^{-2}. The average G flux for the "measured" scenario was 11.89 W m^{-2} with a maximum of 208 W m^{-2}.

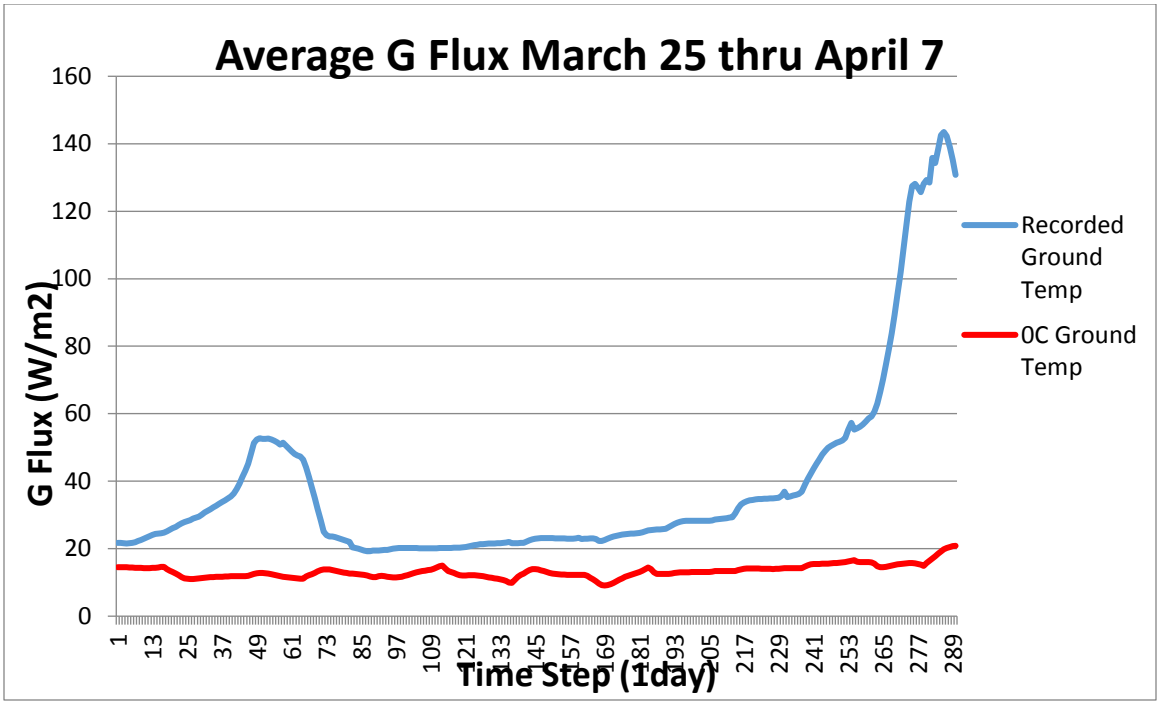

Figure 18 Averaged G Flux (timestep 0 = 3/26 and point 289 = 4/7). This graph shows the last two weeks of the snow covered season and how the G flux changes rapidly with snow depth.

5. DISCUSSION

5.1.1 Ground Temperatures

The flattening of the temperature profiles in Figure 11 and 12 indicate the period with a persistent insulating snowpack on the ground. In Figure 12 at the 2cm depth there is a dip in the temperature profile in mid December. This likely occurred due to a shallow non-insulating snowpack. The air temperatures were colder at this higher elevation site and resulted in colder ground temperatures. In Figure 11, both temperature profiles at 2cm and 10cm start colder and gradually increase in temperature and then level off. This gradual increase in temperature results from the insulating characteristics of the snowpack above, gradually warming the ground below by slowing down radiative heat loss. Towards the end of the snow covered season the temperature profile begins to decline back towards zero. This decline in temperature is a result of snowpack ripening when cold melt water hits the ground surface and the snow depth decreasing.

On 2/12/16 percolation columns were noted in the top 20cm in a snow profile at the lower weather station. This was the onset of snowpack ripening indicated by the snow profile in Figure 19. The upper layer in the snow profile (40cm-43cm) consisted of wet snow grains that had gone through multiple melt freeze cycles. The under lying layer (43cm-28cm) was frozen at the time of inspection, but also consisted of melt freeze grains which meant that melt/freeze cycles were occurring. Under closer inspection, there were also percolation columns indicating that melt near the surface was moving downward through the snowpack.

The next visit to the site was on 2/19/16 and a fully isothermal snowpack had developed, which is a condition that needs to be met in order for melt water to be generated at the base of the snowpack. Ground temperature data in Figure 11 reflect the ripening process as the temperatures begin to decline. Inspection of collected soil moisture data showed an increase in moisture content during the onset of the isothermal conditions. On 2/21/16 ground temperature sensors showed an expected lag in response to increased soil moisture. The temperatures began to decrease and approach 0°C as the snowmelt percolation cooled the warm insulated soils. This trend continued until the snow was completely melted around 2/28/16.

It is possible that the early onset of the 2015/16 snow season allowed for the ground temperatures to be warmer throughout the winter season. Early season snowfall in the Jemez Mountains allowed for insulation of warmer ground temperatures and preserved those temperatures through the snow covered season. If there was a lack of insulating snow cover, for example into December, the ground would have likely frozen from very cold air temperatures in December and the heat flux would likely be different.

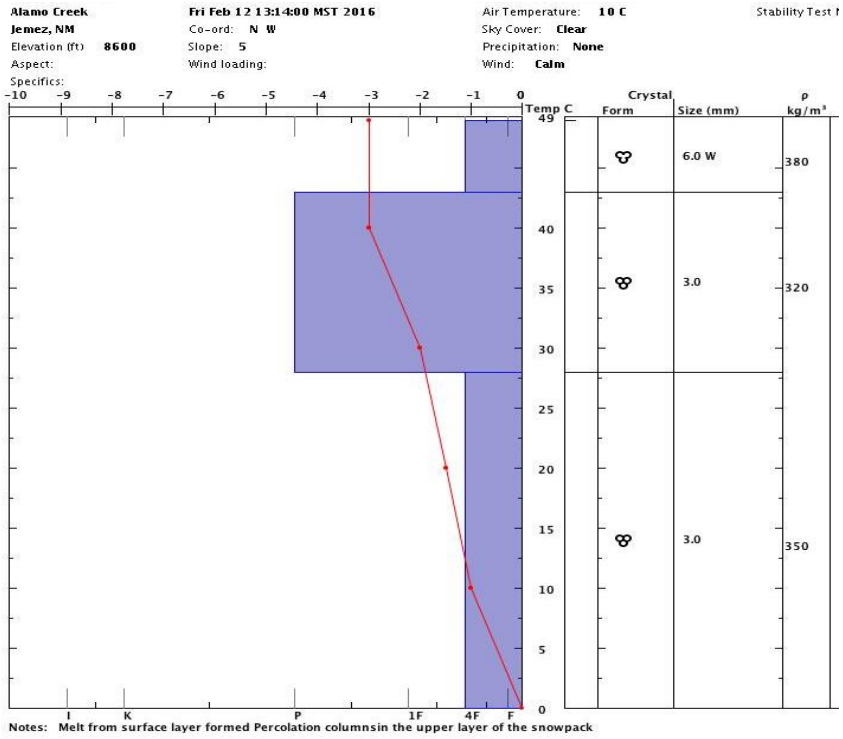

Figure 19. Snow Profile Lower Alamo Creek with wet melt grains throughout the height of the snowpack indicating snowpack ripening.

5.1.2 Snow Presence and Disappearance

Previous studies by Schmid *et al.* (2012) noted that detection of snowpack presence and disappearance was only detectable with an insulating snowpack, which is defined as 25cm or greater. When comparing the HOBO temperature sensor footprints for detection of snowpack presence and disappearance, near surface temperature sensors appeared to perform very well. The seasonal snowpack was easily detectable, for example in Figure 10 by the dampening in temperature fluctuations. All sites showed a similar trend and were very close to representing the presence of snow cover.

Precipitation in the form of snow was also represented well by these near surface temperature sensors. Although there was under 25cm of snow cover, the dampening of the near

surface temperature sensors was clear. This combined with field observations allow for high confidence in the presence of shallow snow and its detectability.

Detecting the snowpack ripening date was less certain. Schmid *et al.* (2012) observed that snowpack ripening occurs when the near surface ground temperatures are warmed to 0℃. Looking at Figure 10 snow pack ripening date would have occurred on 3/1, however field observations on 2/19 showed a near ripe snowpack. Further measurements combined with easily accessible field sites could help improve this theory.

5.1.3 Calculated Ground Heat Flux

On all dates and locations, the ground/snow interface temperatures were below $0°C$ except at the lower weather station on 2/12. Typically the ground/snow interface temperature is assumed $0°C$ for modeling the snowpack energy balance. The ground temperatures below the ground were above $0°C$ throughout the course of the winter once a seasonal snowpack was present even at the most shallowly buried temperature sensors. Furthermore, measured near soil/snow interface temperatures throughout the winter season were generally below 0℃.

At the Upper Weather Station G flux was slightly lower on 1/18/16 than mid-season, likely as a result of snowpack depth and a shorter duration of snow cover compared to measurements thereafter. The ground was still cooler than under mid-season conditions. When the ground temperature is cooler the G value will be less.

The G value was highest during mid-winter on 2/12/16 when the snowpack was deepest at the upper weather station allowing for gradual warming of the ground temperatures, which ultimately increased the G value. On 3/17/16 the snowpack started to show signs of melting near the snow surface, however not at the bottom of the snowpack. The ground temperature began to

cool slightly compared to the previous measurements. This could be a result of the decreasing snowpack height. As the temperature of the ground started to cool, the G value also decreased.

The lower weather station site showed similar trends to the upper weather station values. In early February the snowpack at the lower weather station was at its maximum average depth. This allowed for the largest amount of insulation to the ground temperature sensors from the snowpack. The temperatures underground were able to warm, resulting in an increased G value.

The G value showed a decrease on 2/12/16 because the K_g value was altered from soil moisture changes as a result of snowmelt reaching the ground surface, ultimately changing the temperature within the ground and at the ground/snow interface.

Given the decreasing trend at both weather stations of the below ground temperatures combined with increasing soil moisture as snowmelt increases, the highest amount of energy received into the base of the snowpack based on equation 9 and using data available from snow pits was during mid-season when ground temperatures were warmest. The below ground temperatures at both weather station footprints showed a fairly constant temperature throughout the snow covered season. The decrease in ground temperatures during the ripening process will decrease the temperature gradient between the ground and snow, as a result, decrease the G value incident to the base of the snowpack.

A limitation of equation 9, which was used for the previously discussed G values is that the soil temperature measurement depth will effect the value of the G flux. This occurs because the temperature gradient will decrease as space is increased.

Depending on which sensor depth was used for calculations, the G flux changes. The temperature differences between sensors buried 10cm to 2cm was generally as small as $.5°K$.

However, changing the depth during calculations with equation 9, the G component would increase when using temperatures closer to the soil/snow interface. Table 7 shows the variance of the G value compared to the depth of the temperature measurement. The closer the ground temperature measurement is to the soil/snow interface, the more accurately the G flux to the base of the snowpack is captured (Lamontagne, 2009). This is the reason the 2cm depth temperatures were used to calculate the G flux into the base of the snowpack even though this resulted in a higher G flux with equation 9. To minimize the effect of the G flux variance, equation 8 was used to compare these calculations.

Date	Location	Moisture %	Tg (K)	Tsbase (K)	z2 (m)	G (W/m2)
1/18/16	Low wx	36.7	274.37	272.65	0.1	21.18
1/29/16	Low wx	36.7	274.37	272.65	0.1	21.18
2/12/16	Low wx	40.5	274.26	273.15	0.1	14.12
1/18/16	Low wx	36.7	273.86	272.65	0.02	74.52
1/29/16	Low wx	36.7	273.88	272.65	0.02	75.70
2/12/16	Low wx	40.5	273.71	273.15	0.02	35.75

Table 7. G Flux Comparison by depth using equation 9 where the G flux was compared by changing the distance between the two measurement points. Changing the distance between the measurement points had an impact on the G flux values. Moving them closer together increased the G flux value.

One other factor that equation 9 was very sensitive to was changing the temperature at the snow/soil interface. Table 8 shows the variance in the G flux based on changing the temperature at the snow/soil interface. By setting the ground temperature at 0℃ the G fluxes were lower than when set to −1℃. The interface temperatures were below 0℃ for each measurement made during snow profile data collection. Using equation 9 and assuming 0℃

temperatures at the snow/soil interface will result in very different G flux values. It was important to check the sensitivity in this equation to small temperature changes because the G flux changes roughly by 144% with a 1℃ temperature change. This method for calculating the G flux gives low confidence in the accuracy of the values obtained.

Low Weather Station		**G Flux at 0℃ (W/m2)**	**G Flux at -1℃ (W/m2)**
1/18/16	Low wx	43.75	105.29
1/29/16	Low wx	41.47	103.01
2/12/16	Low wx	35.75	99.24
Upper Weather Station			
1/18/16	Upper wx	13.76	70.84
2/12/16	Upper wx	19.58	76.66
3/17/16	Upper wx	13.24	70.33

Table 8. G Flux variance with snow/soil interface temperatures varying from 0℃ to -1℃ showing the sensitivity of temperature to equation 9

As previously mentioned, equation 8 treats the upper soil layer and the lower snow layers as homogenous. When using this interface as a single layer, it is assumed that heat transfer is uniform throughout his layer. The G flux into the base of the snowpack is calculated in Table 4

Table 4 shows the differences in the G flux value depending on the time of year as well as reflecting changes in the snowpack depth. The G flux was greater at the lower weather station likely as a result of the lower elevation and south facing aspect receiving more solar radiation. Also, thick grass vegetation above the ground could help enhance insulation of the ground surface. The G value at the lower weather station also decreased during the snowpack ripening process due to cold snowmelt water infiltrating into the ground surface cooling the

temperatures at that depth. As the temperature is cooled underground the G flux decreases due to a declining temperature gradient.

Equation 8 was also tested for sensitivity to the parameters that go into calculating the G flux value. The first sensitivity analysis was checked by changing the soil moisture, which will change the effective thermal conductivity values. By raising the soil moisture from 18% to 40%, the value K_{eg} was raised from 1.33 to 1.7 W m^{-2}. The change in K_{eg} only increased the G flux from 10.31 to 10.39 W m^{-2}.

The depth of the soil temperature measurement was also checked and was changed from 2cm to 10cm. By changing the depth from 2cm to 10cm the temperature gradient is spread further resulting in a lower G flux, however the change was minimal from 10.31 to 9.05 W m^{-2}.

The next parameter that was tested for sensitivity in equation 8 was the ground temperature. The range of values during the snow covered season at 2cm depth was . 2℃ to .8℃ at the upper weather station site. Setting the temperature at . 2℃ resulted in a G flux of 10.31 W m^{-2}. Setting the ground temperature at the higher value of .8℃ resulted in a G flux value of 12.88 W m^{-2}. One final test of sensitivity, the ground temperature was set at 2℃, which by all measured values is an unreasonable value. The G flux value still only slightly changed to 18.86 W m^{-2}.

Snow temperatures were also tested for sensitivity using equation 8. Changing the temperature at 10cm from -2℃ to -1℃ changed the G flux from 10.3 to 5.7 W m^{-2}. Changing the depth of this temperature measurement showed the greatest sensitivity. The snow temperature depth was measured at 10cm and when changing the depth to 5cm the G flux value changed from 10.31 to 19.93 W m^{-2}.

Overall, the G values decreased when using equation 8 compared to equation 9. This occurred because it takes into account for snowpack conditions. Equation 9 only uses soil characteristics to generate a G flux values. Completing the sensitivity analysis of these two equations was important to recognize the limitations. Equation 9 is far more sensitive than equation 8. By including snow and soil characteristics as well as other physically based parameters such as effective thermal conductivity of soil and snow, equation 8 does a better job of calculating the G flux values as it removes much of the sensitivity that limits equation 9.

After completing the sensitivity analysis of equation 8, confidence is much higher in the values produced by this equation compared to equation 9. Multiple parameters were adjusted and tested using equation 8 which resulted in minimal changes to the values obtained for G fluxes. Using equation 9 could over estimate the G flux amount into the base of the snowpack. Or, if temperatures deeper underground are used for the calculation, equation 9 could under estimate the G flux value.

5.1.4 Model Validation

In order to test the model that was calibrated using the methods previously described, validation of this calibration was tested at the lower weather station site. In order to validate the model, results at the lower weather station site should be similar to measured snow depths at this location with minimal adjustments made to the inputs. The adjustments that were made to the lower weather station model run were minimal. The first adjustment to the model was the elevation in which the model was run at. The second adjustment to the model run was to input the precipitation amount at the lower site. The final adjustment that was made was inputting the measured ground temperatures at the lower weather station. All other parameters were held constant from what was calibrated at the upper weather station model run.

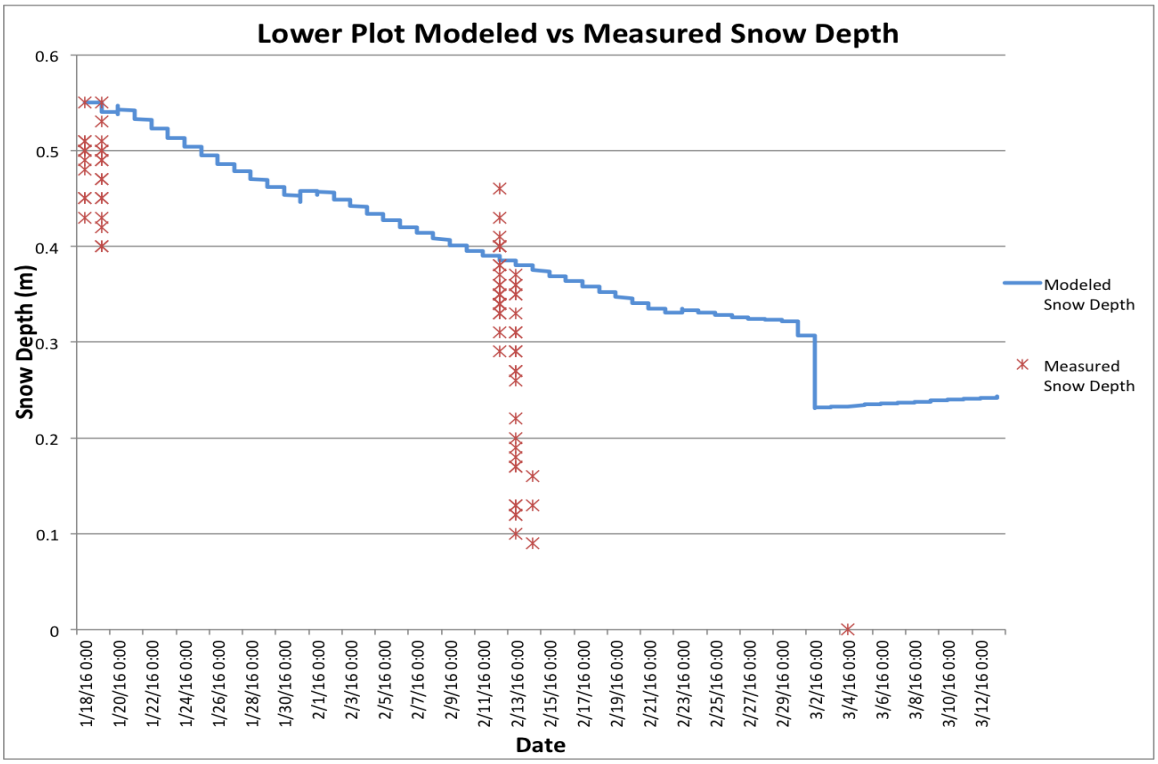

Figure 20. Lower Weather Station Modeled Snow Depth vs Measured Snow Depth. Snow depth measurements from snow course transects were done on 1/18 and 2/12. On 3/4 snow was gone.

Figure 20 shows the modeled snow depth in blue against the measured snow depths at the lower weather station snow course site. The markings in red are the snow depth distribution along the snow course and represent the variability in snow depth and space.

Looking at Figure 20, the model passes through the measured snow depth and falls within the range of measurements made at this site, much like the calibrated model for the upper weather station. One major drawback to the SNOBAL model calibration and validation is the lack in variability of snow depth throughout the season. In other words, there were not many ups and downs in the snow depth throughout the season to effectively test the performance of the model. Using the span of snow depths at the upper weather station allowed for a fairly easy target to hit for calibration. Perhaps using the average snow depth would have been a better target to aim for.

There are only a couple parameters while tuning SNOBAL that have an effect on the output. Shortwave and longwave radiation had the largest effects on the output of the model. SNOBAL was not sensitive to precipitation adjustments as seen in the Figure 13. Making relatively large increases in precipitation still had a limited effect on the snow depth from the model. Using this model would be difficult if the snow depth changed frequently from snow accumulation. Increasing the amount of precipitation as well as the density of the precipitation still had little effect on the snow depth of the model output. Model confidence is low in relation to snow depth changes resulting from snow accumulation.

The snow disappearance during the model validation is also not represented accurately by this model run in Figure 20. The snow was melted around March 1 as indicated by near surface temperatures. This model run does not melt the snowpack fast enough. If solar radiation numbers from this site were input, which were as high as 850 W m^{-2} the snowpack would likely melt on time. As previously mentioned, SNOBAL was very sensitive to net radiation tuning and minimal adjustments to those numbers would allow significant changes in the model output.

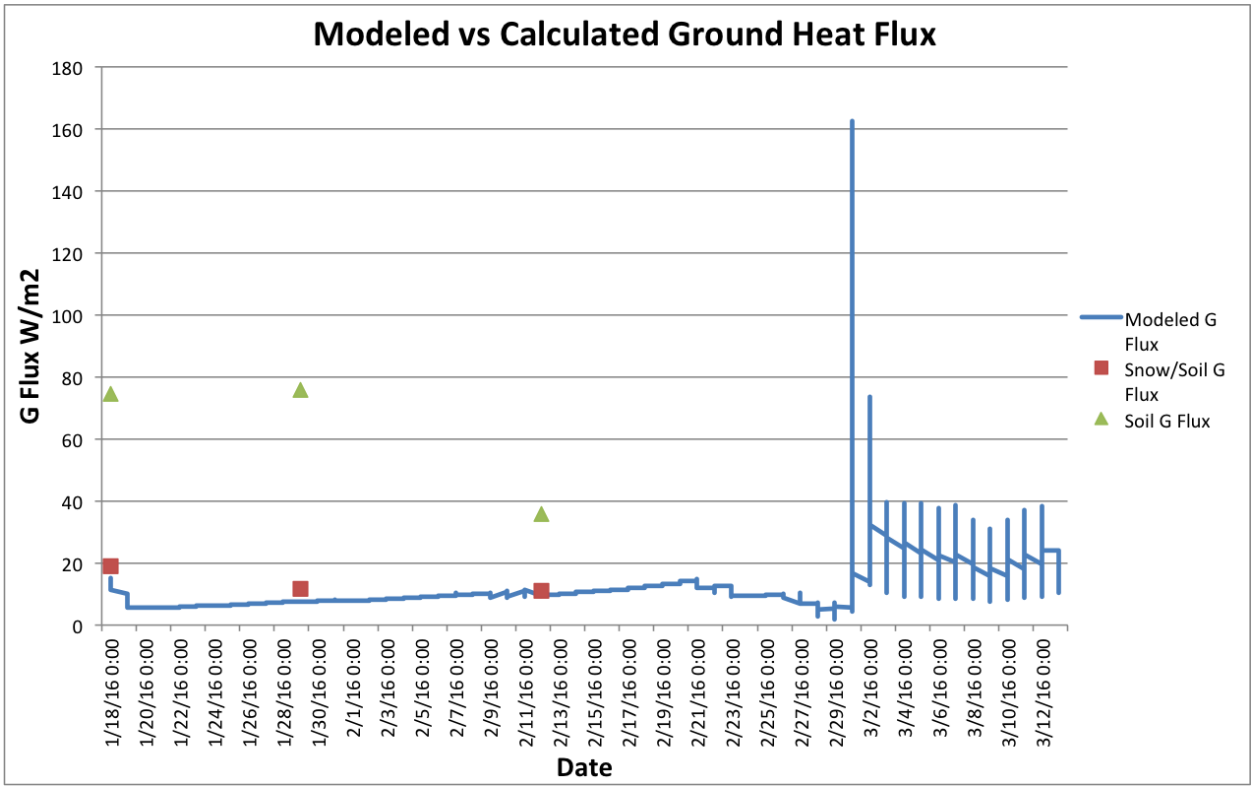

Figure 21 Modeled and Calculated G Flux

Further model validation was tested through investigation of calculated and modeled G fluxes shown in Figure 21. Similar to the upper site model, the lower site model compared well to G flux calculations using equation 8, which values are represented in red. The green values in Figure 21 were calculated using equation 9 and again do not compare well to the modeled results.

Both the upper and lower site models had similar G flux values throughout the snow covered season generally between 5 and 18 W m^{-2}. Both sites also showed an increase in the G flux as the lower layer of the snowpack within the model disappeared leaving the active layer of 25cm in depth. Validation of the calibrated SNOBAL model appeared most effective for the G flux values. Snow depth validation is suspect given the large target being used to calibrate.

5.1.5 Model Scenario

The results during the three model scenario focusing on the effects of the ground temperature tuning was important in order to see how the G flux in the semi-arid mountain climate of the Jemez Mountains might vary compared to other mountain locations in different climates. The SNOBAL model was not overly sensitive to G flux tuning, however, did have an effect indicated by the G flux modeling scenario.

Given the accuracy and correlation of the G flux model results to the calculated model results, confidence is high in the G flux values generated by the model. Confidence is also high regarding the G flux numbers because the G flux calculations were based off of independent field measurements such as snowpack layer densities, soil moisture characteristics and types.

The findings during this study show a difference in snowpack evolution as indicated by the three model scenario and should be considered during future modeling work. The typical 0℃ assumption is not the most accurate in this climate, also indicated by work in Arizona. The results from this study showed a higher G flux value than the 0℃ scenario throughout the entire snow covered season, with a large increase in the G flux during the end of the season.

This result is important to consider when looking into how the energy balance might change with climate change. This late season flux might actually decrease if snow covered seasons become shorter and snowpacks melt earlier in the year. If the snowpack melts earlier in the year then the solar radiation might not be as intense and keep the G flux slightly lower during the final ablation period. However, under climate change, if snowpacks become generally shallower, there might be a season long increase in the G flux from increased interaction of solar radiation penetrating to the ground surfaces.

When considering the importance of the G flux, melt generation was also looked at to see which scenario was generating a greater amount of melt from the snowpack as a result of higher G flux values. The "0℃" scenario had a total melt of 194.2 kg m^{-2} where the "measured" scenario resulted in 317.6 kg m^{-2} of melt. This shows the increased importance that the G flux value has in relation to typical model assumptions for snowmelt. With snowpack process modeling, its important to be able to estimate melt generation. If under estimating the G flux, estimations of melt runoff will likely be misrepresented in terms of quantity and timing.

5.1.6 Energy Exchange

In Table 5 the overall radiation budget per month is shown. In January and February the Q value is negative for both months. This indicates an overall energy loss from the snowpack. The over all energy loss from the snowpack correlates to snow accumulation periods without a lot of melt. This is indicated by the negative net radiation value likely resulting from longwave radiation losses during cold nighttime temperatures.

Sensible heat values are the highest positive values during January and February as the difference in snow surface temperature and air temperature were likely the greatest during this period. Air temperatures were warmer than the snowpack surface allowing for sensible heat exchange to the snowpack surface. This result is supported by Hawkins *et al.* where the air temperature was warmer than the snow temperature due to the snow's high emissivity and the additional cooling factor associated with the sublimation and evaporation that were occurring from the snowpack (2007).

Average and maximum G flux values in Tables 5 and 6 generally increased throughout the season, with the largest increases occurring towards the end of the snow covered season. The

contribution of the G flux during the first week in April became higher than the net radiation term for the first time. Maximum G flux values in March and April increased significantly compared to January and February and shows the significance of the G term especially during the ablation period.

The M contribution to the snowpack was minimal when it existed, and for March and April there was no advection term. M was low because there was no precipitation added to the snowpack. The advection term was positive in January and February indicating snow accumulation. If the advection term was negative there would have been advection losses resulting from rain on snow events, which did not occur.

Table 9 shows the comparison of G flux percentage during the time period in which it was measured for different study regions. The Happy Jack Flats G flux was measured during the snow covered season. Due to the timing of the snow covered season at Happy Jack, AZ the G flux is likely lower because the snow disappears in early February. Given the early melt at this location, there is still a significant difference between this location and deeper snowpack areas.

The Niwot and Emerald Lake sites were measured during the melt period of the snowpack, which should give higher G fluxes, however is still a very small component to the ablation process as indicated by the percent contribution in Table 5. The Jemez Mountain site shows a seasonal average G flux of 26 percent, greater than all other sites. The increase in the G flux contribution at this location correlates to the increase in net radiation percentages. The net radiation percentage is increasing because solar radiation is increasing. The G flux value is likely increasing because of more atmosphere and ground interaction.

Location	Elevation (ft)	Dates	G Flux %
Happy Jack, AZ	7672	12/31-2/6, 2003	18
Niwot Ridge, CO	11606	4/25-6/6, 1997	3
Emerald Lake, CA	10180	5/1-5/31,1986	1
Alamo Border, NM	9780	1/18-4/7/2016	26

Table 9. G flux percent per site location taken from previous studies. Alamo Border had the highest percent contribution.

6. Conclusions

As snowpacks begin to shrink and snow covered seasons shorten, it is important to understand how shallower snowpacks combined with shorter durations might impact the energy budget. The overall goal of this research was to collect snowpack data, ground temperature data, and meteorological data in order to model snowpack and energy balance processes using SNOBAL. One objective was to compare ground heat flux calculations to modeled ground heat flux values. Additional objectives of this research were to investigate the significance of the ground heat flux in this semi-arid mountain environment compared to more studied climate regions and also determine if near surface soil temperatures could indicate snow presence and disappearance.

Depending on the method used for calculating the G flux values, the resulting numbers very different. When using the equation that does not account for the snowpack characteristics, the G flux values changed as the distances changed from the soil/snow interface. Using the equation that combines the lower snowpack characteristics and soil characteristics produces

smaller G flux values through mid winter and align to modeled G flux values. The alignment of calculated and modeled G flux values gives high confidence in the model results for the G flux.

While examining the modeled energy balance of the snowpack the most significant difference compared to other studied regions was the contribution of the G flux. The G flux value was far more significant in this climate during the snow covered season accounting for 26% of the energy flux of the snowpack. Using the assumed 0℃ ground temperature did not prove a significant enough energy flux to melt the snowpack in the time it took for it to melt out. This could be an important consideration for future modeling within this semi-arid region with shallow snowpacks.

The final objective of this research was to try to determine if ground temperatures could be used to determine the presence of snow cover. Using the near surface ground temperatures and comparing them to field observations, it was reasonable to determine the snow covered season. The insulating effect of the snow cover allowed for a dampening of diurnal temperature fluctuations of the near surface ground temperatures. This observation made it possible to determine the presence of snow on the ground.

6.1.1 Recommendations for Future Work

Additional observations would provide more information on the assumptions and conclusions that were made during this study. The winter snow accumulated earlier than usual allowing for warmer ground to be insulated by snow cover, which could ultimately increase the seasonal ground heat flux value. A later onset to the snow covered season might allow ground temperatures to cool more significantly and change the ground heat flux. Inspection of the G flux under La Nina snowpack condition would be informative for this conclusion.

Another thing to help increase the accuracy of the model and calculated ground heat fluxes would be to collect snowpack temperatures all season long. Spacing temperature sensors 10cm vertically throughout the snowpack for the duration of the season could help improve confidence. This would help calculate more points to compare the model to instead of just using snow profile data, which was limited temporally because it was time consuming to complete given the 13 mile round trip ski every time the data needed to be collected. Having more measured data to calculate the G flux during the end of the season G flux increase would give better confidence in the model as well. Information could be gained by seeing if the model is over representing the G flux at the end of season by comparing calculated values from measured data.

Measuring the solar radiation reaching the ground surface would be a good way to see if there is an increase in ground/atmosphere interaction. The recorded ground temperatures did not reflect this increase in radiation as expected. Setting up a way to measure radiation reaching the ground surface would be a good way to understand the solar interaction with the ground surface under the snowpack.

Additional research should be investigated in order to observe the actual ripening date based on near surface ground temperatures. Having the ability to easily and quickly access a field site to observe snowpack characteristics during the melt season would allow for the careful inspection of the exact ripening date. This would allow for better validation of ground temperatures and the ability to correlate them to the ripening day. Furthermore, additional research that could span from using ground temperature data would be a range scale project to track snow distribution changes over time using buried temperature sensors.

7. References

Allen, Jason, T. Darden, R. Floyd, M. Gallaher, D. Jones, K. Kostelnik, K. Kretz, R. Lucero, B. Musick. R. Romero, B. Toth, M. Uhl, L. Weaver. (2005). *Potential Effects of Climate Change on New Mexico.* Agency Technical Work Group State of New Mexico.

Anderson, E. (1976). *A point energy balance model of snow cover*. NWS Tech. Rept. 19, 150 pp. Nat. Oceanic and Atmos. Admin, Washington, D.C

Anderton, S. P., White, S. M., & Alvera, B. (2004). Evaluation of spatial variability in snow water equivalent for a high mountain catchment. *Hydrological Processes*, *18*(3), 435-453.

Anderson, E. (2006). *Snow Accumulation and Ablation Model SNOW-17.* Retrieved from http://www.nws.noaa.gov/oh/hrl/nwsrfs/users_manual/part2/_pdf/22snow17.pdf.

Bales, R. C., Molotch, N. P., Painter, T. H., Dettinger, M. D., Rice, R., & Dozier, J. (2006). Mountain hydrology of the western United States. *Water Resources Research*, 42(8).

Baker, D. G., Skaggs, R. H., & Ruschy, D. L. (1991). Snow depth required to mask the underlying surface. *Journal of Applied Meteorology*, *30*(3), 387-392.

Boike, J., Roth, K., & Ippisch, O. (2003). Seasonal snow cover on frozen ground: Energy balance calculations of a permafrost site near Ny-Ålesund, Spitsbergen. *Journal of Geophysical Research: Atmospheres (1984–2012)*, *108*(D2), ALT-4.

Cline, D. W. (1997). Snow surface energy exchanges and snowmelt at a continental, midlatitude Alpine site. *Water Resources Research*, *33*(4), 689-701.

Colbeck, S. C. (1982). An overview of seasonal snow metamorphism. *Reviews of Geophysics*, *20*(1), 45-61.

Deems, J. S., Fassnacht, S. R., & Elder, K. J. (2006). Fractal distribution of snow depth from LiDAR data. *Journal of Hydrometeorology*, *7*(2), 285-297.

Deems, J. S., Fassnacht, S. R., & Elder, K. J. (2008). Interannual consistency in fractal snow depth patterns at two Colorado mountain sites. *Journal of hydrometeorology*, *9*(5), 977-988.

DeWalle, D. R., & Rango, A. (2008). *Principles of snow hydrology*. Cambridge University Press.

Dozier, J., & Painter, T. H. (2004). Multispectral and hyperspectral remote sensing of alpine snow properties. *Annu. Rev. Earth Planet*. Sci., 32, 465-494.

Dunne, T., & Black, R. D. (1971). Runoff processes during snowmelt. *Water Resources Research*, 7(5), 1160-1172.

Elder, K., Dozier, J., & Michaelsen, J. (1991). Snow accumulation and distribution in an alpine watershed. *Water Resources Research*, *27*(7), 1541-1552.

Erxleben, J., Elder, K., & Davis, R. (2002). Comparison of spatial interpolation methods for estimating snow distribution in the Colorado Rocky Mountains. *Hydrological Processes, 16*(18), 3627-3649.

Farouki, O. T. (1981). Thermal properties of soils (No. CRREL-MONO-81-1). Cold Region Research And Engineering Lab Hanover, NH.

Flerchinger, G. N., & Saxton, K. E. (1989). Simultaneous heat and water model of a freezing snow-residue-soil system I. Theory and development. *Trans. ASAE, 32*(2), 565-571.

Granger, R. J., & Male, D. H. (1978). Melting of a prairie snowpack. *Journal of Applied Meteorology, 17*(12), 1833-1842.

Greene, Ethan, D. Atkins, K. Birkeland, K. Elder, C. Landry, B. Lazar, I. McCammon, M. Moore, D. Sharaf, C. Sternenz, B. Tremper, and K. Williams. (2010). Snow, Weather and Avalanches: Observation Guidelines for Avalanche Programs in the United States. American Avalanche Association Pagosa Springs, CO/

Harpold, A., Brooks, P., Rajagopal, S., Heidbuchel, I., Jardine, A., & Stielstra, C. (2012). Changes in snowpack accumulation and ablation in the intermountain west. *Water Resources Research*, 48(11).

Harpold, A. A., Biederman, J. A., Condon, K., Merino, M., Korgaonkar, Y., Nan, T., ... & Brooks, P. D. (2014). Changes in snow accumulation and ablation following the Las Conchas Forest Fire, New Mexico, USA. *Ecohydrology, 7*(2), 440-452.

Hawkins, T. W., & Ellis, A. W. (2007). A case study of the energy budget of a snowpack in the arid, subtropical climate of the southwestern United States. *Journal of the Arizona-Nevada Academy of Science*, 39(1), 1-13.

Hodgkinson, RA. (2004). Evaluation of Tipping Bucket Rain Gauge Performance and Data Quality. Environmental Agency Almondsbury, Bristol.

IPCC, 2013: Climate Change 2013: The Physical Science Basis. Contribution of Working Group I to the Fifth Assessment Report of the IntergovernmentalPanel on Climate Change [Stocker, T.F., D. Qin, G.-K. Plattner, M. Tignor, S.K. Allen, J. Boschung, A. Nauels, Y. Xia, V. Bex and P.M. Midgley(eds.)]. Cambridge University Press, Cambridge, United Kingdom and New York, NY, USA, 1535 pp

Lamontagne, Aurele. (2009). Characterization and quantification of ground heat flux for late season shallow snow. MSc Thesis, Hydrologic Sciences, Boise State University, Boise.

Lawrence, M. G. (2005). The relationship between relative humidity and the dewpoint temperature in moist air: A simple conversion and applications. Bulletin of the American Meteorological Society, 86(2), 225-233.

Lehning, M., Bartelt, P., Brown, B., Fierz, C., & Satyawali, P. (2002). A physical SNOWPACK model for the Swiss avalanche warning: Part II. Snow microstructure. *Cold Regions Science and Technology, 35*(3), 147-167.

Lenart, Melanie. 2008. "Southwest Climate Change." The University of Arizona. (retrieved from *http://www.southwestclimatechange.org/)*.

Leavesley GH, Lumb AM, Saindon LG. (1987). A microcomputer-based watershed-modeling and data-management system. Proceedings, 55th Annual meeting, Western Snow Conference, Western Snow Conference, Vancouver, British Columbia, Canada: pp. 108-117.

Liston, G. E., & Elder, K. (2006). A distributed snow-evolution modeling system (SnowModel). *Journal of Hydrometeorology*, *7*(6), 1259-1276.

Lundquist, J. D., & Lott, F. (2008). Using inexpensive temperature sensors to monitor the duration and heterogeneity of snow-covered areas. *Water Resources Research*, *44*(4).

Male, D. H., & Granger, R. J. (1981). Snow surface energy exchange. *Water Resources Research*, *17*(3), 609-627.

Marks, D., Dozier, J., & Davis, R. E. (1988). Climate and energy exchange at the snow surface in the alpine region of the Sierra Nevada: 1. Meteorological measurements and monitoring. *Water Resources Research*, *28*(11), 3029-3042.

Marks, D., Dozier, J., & Davis, R. E. (1992). Climate and energy exchange at the snow surface in the alpine region of the Sierra Nevada: 1. Meteorological measurements and monitoring. *Water Resources Research*, *28*(11), 3029-3042.

Marks D, Dozier J. (1992). Climate and energy exchange at the snow surface in the alpine region of the Sierra Nevada: 2. Snow cover energy balance. *Water Resources Research 28*: 3043-3054.

Marks, D., Kimball, J., Tingey, D., & Link, T. (1998). The sensitivity of snowmelt processes to climate conditions and forest cover during rain on snow: a case study of the 1996 Pacific Northwest flood. *Hydrological Processes*, *12*, 1569-1587.

Marks, D., Domingo, J., Susong, D., Link, T., & Garen, D. (1999). A spatially distributed energy balance snowmelt model for application in mountain basins. *Hydrological Processes*, *13*(12-13), 1935-1959.

Marks, D., & Winstral, A. (2001). Comparison of snow deposition, the snow cover energy balance, and snowmelt at two sites in a semiarid mountain basin. *Journal of Hydrometeorology*, *2*(3), 213-227.

McClung, D., & Schaerer, P. A. (2006). *The avalanche handbook*. The Mountaineers Books.

McDaniel, Paul. (n.d.) *The Twelve Soil Orders.* University of Idaho, Moscow. Retrieved from http://www.cals.uidaho.edu/soilorders/mollisols.htm

Ministry of the Environment. 1981. Snow Survey Sampling Guide. Surface Water Section Water Management Brach, Victoria British Columbia.

Muldavin, Esteban, P. Tonne. (2003). *A Vegetation Survey and preliminary Ecological Assessment of Valles Caldera National Preserve, New Mexico*. University of New Mexico

Romero, Chris. (2016). *Water Supply Forecast for New Mexico*. Natural Resources Conservation Services, Albuquerque, NM. Retrieved from http://www.nrcs.usda.gov/wps/portal/nrcs/detail/nm/snow/waterproducts/?cid=nrcs144p2_068877

Schmid, M. O., Gubler, S., Fiddes, J., & Gruber, S. (2012). Inferring snowpack ripening and melt-out from distributed measurements of near-surface ground temperatures. *The Cryosphere*, *6*(5), 1127-1139.

Şensoy, A., Şorman, A. A., Tekeli, A. E., Şorman, A. Ü., & Garen, D. C. (2006). Point-scale energy and mass balance snowpack simulations in the upper Karasu basin, Turkey. *Hydrological processes*, *20*(4), 899-922.

Smith, R., Moore, D., & Weiler, M. (2007, December). Midwinter Snowmelt Generated by Ground Heat Conduction: Implications for Catchment Hydrology. In *AGU Fall Meeting Abstracts* (Vol. 1, p. 0636).

Smith, R. S., Moore, R. D., & Weiler, M. (2008, December). Spatio-temporal variability in midwinter snowmelt generated by ground heat flux: implications for catchment hydrology. In *AGU Fall Meeting Abstracts* (Vol. 1, p. L05).

Soil Survey Staff, Natural Resources Conservation Service, (n.d). United States Department of Agriculture. Web Soil Survey. Available online at http://websoilsurvey.nrcs.usda.gov/. Accessed [6/1/2016].

Sturm, M. (2015). White water: Fifty years of snow research in WRR and the outlook for the future. *Water Resources Research*, *51*(7), 4948-4965.

Tyler, S. W., Burak, S. A., McNamara, J. P., Lamontagne, A., Selker, J. S., & Dozier, J. (2008). Spatially distributed temperatures at the base of two mountain snowpacks measured with fiber-optic sensors. *Journal of Glaciology*, 54(187), 673-679.

University Corporation for Atmospheric Research. (2007). Snow Albedo. Retrieved from https://www.meted.ucar.edu/hydro/basic/Snowmelt/ on 8/5/2016.

Vionnet, V., Brun, E., Morin, S., Boone, A., Faroux, S., Le Moigne, P., ... & Willemet, J. M. (2012). The detailed snowpack scheme Crocus and its implementation in SURFEX v7. 2. *Geoscientific Model Development*, *5*, 773-791.

Wakahama, G. (1968). The metamorphism of wet snow. *IAHS Publication*, *79*, 370-379.

Wankiewicz, A. (1979). A review of water movement in snow. Hanover, NH, U.S. Army Corps of Engineers. Cold Regions Research and Engineering Laboratory, 222-252.

Woo, M. K., & Heron, R. (1981). Occurrence of ice layers at the base of High Arctic snowpacks. *Arctic and Alpine Research*, 225-230.

Zhang, T. (2005). Influence of the seasonal snow cover on the ground thermal regime: An overview. *Reviews of Geophysics*, *43*(4).